

Nuclear Density Functional Theory for Astrophysics

PART II– Nuclear weak interaction processes

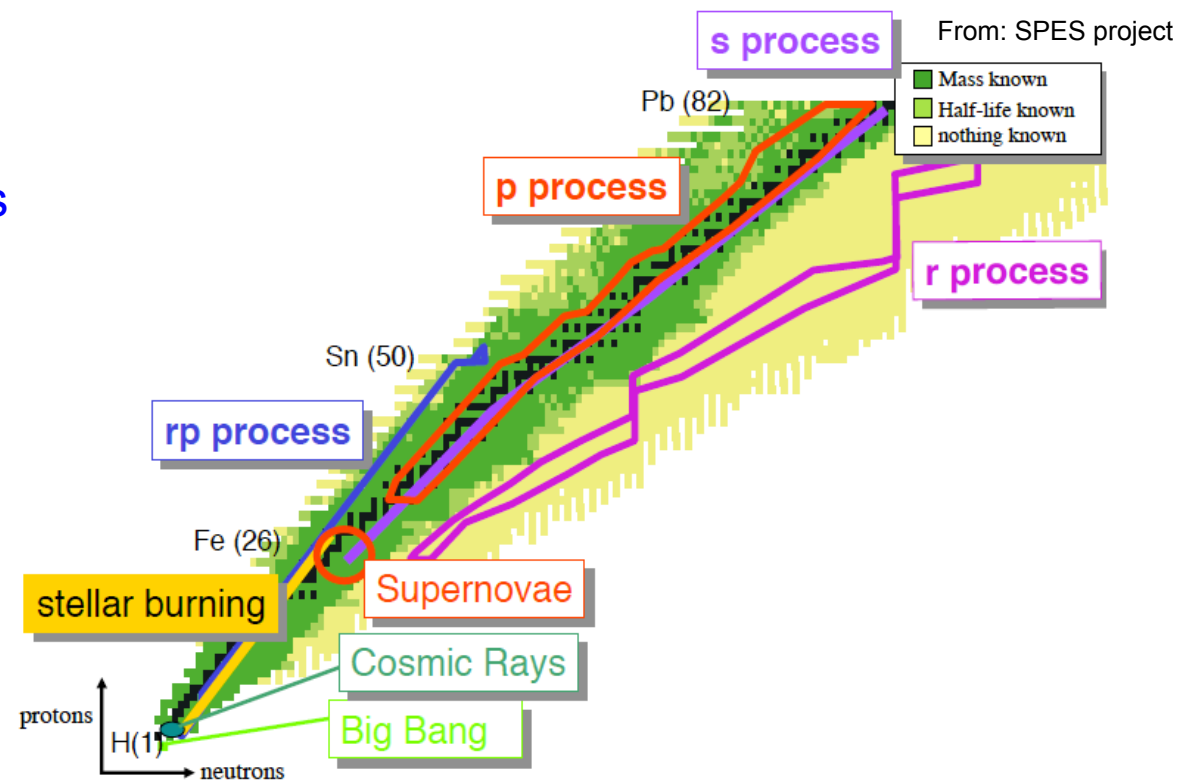
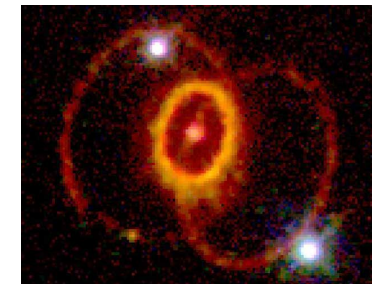
N. Paar

Department of Physics, Faculty of Science, University of Zagreb, Croatia

INTRODUCTION

- Accurate nuclear physics information is essential for understanding the evolution of stars and nucleosynthesis
- Relevant nuclear processes in presupernova stellar collapse and at later stages of supernova evolution

- electron capture
- beta decay
- neutrino-nucleus reactions
- neutron capture
- photodissociation
- fission
- ...



NUCLEAR THEORY FOR ASTROPHYSICS

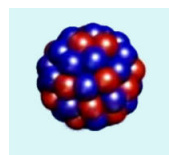
So far, a variety of nuclear theory inputs have been used in astrophysical / nucleosynthesis simulations...



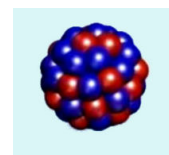
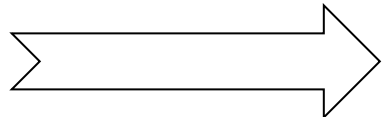
Final understanding of how supernova explosions and nucleosynthesis work,
with self-consistent microscopic description of all relevant nuclear physics included,
has not been achieved yet.

Theoretical uncertainties in nuclear properties are mainly unknown.

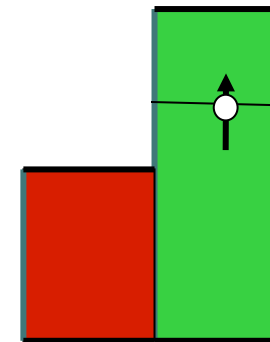
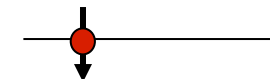
NUCLEAR SPIN-ISOSPIN TRANSITIONS



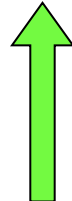
Z, N



$Z+1, N-1$



$$|GTR\rangle = S_- T_+ |Z, N\rangle$$



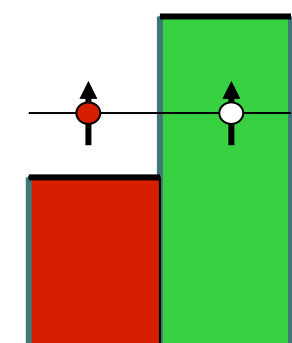
spin flip σ

$|Z, N\rangle$



$|IAR\rangle = T_+ |Z, N\rangle$

isospin flip τ

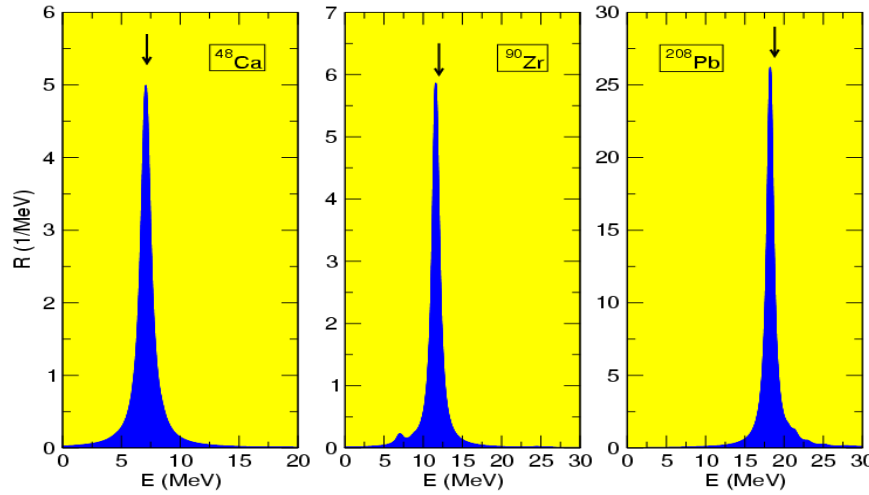


p n

IAR – Isobaric Analogue Resonance
GTR – Gamow-Teller Resonance

$|p\rangle \equiv |t = 1/2, t_3 = +1/2\rangle$
 $|n\rangle \equiv |t = 1/2, t_3 = -1/2\rangle$

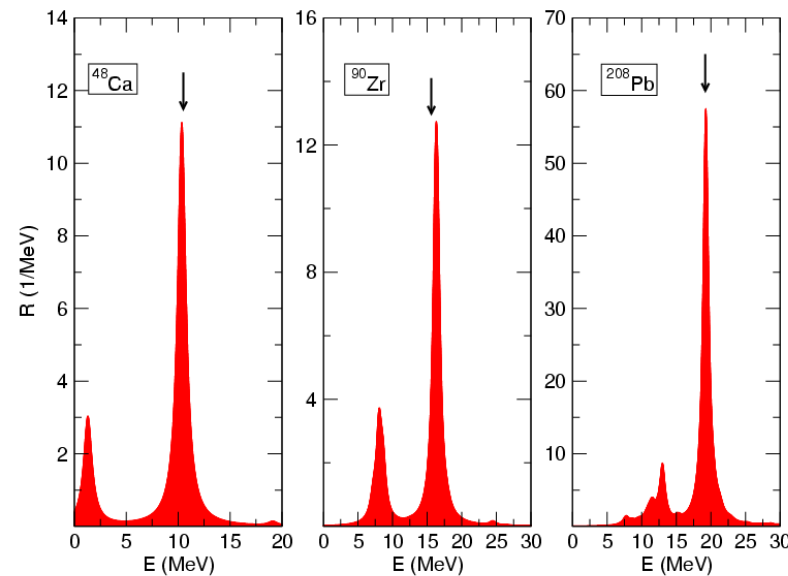
NUCLEAR SPIN-ISOSPIN TRANSITIONS



Model calculations based on the relativistic (quasiparticle) random phase approximation

ISOSPIN-FLIP
EXCITATIONS

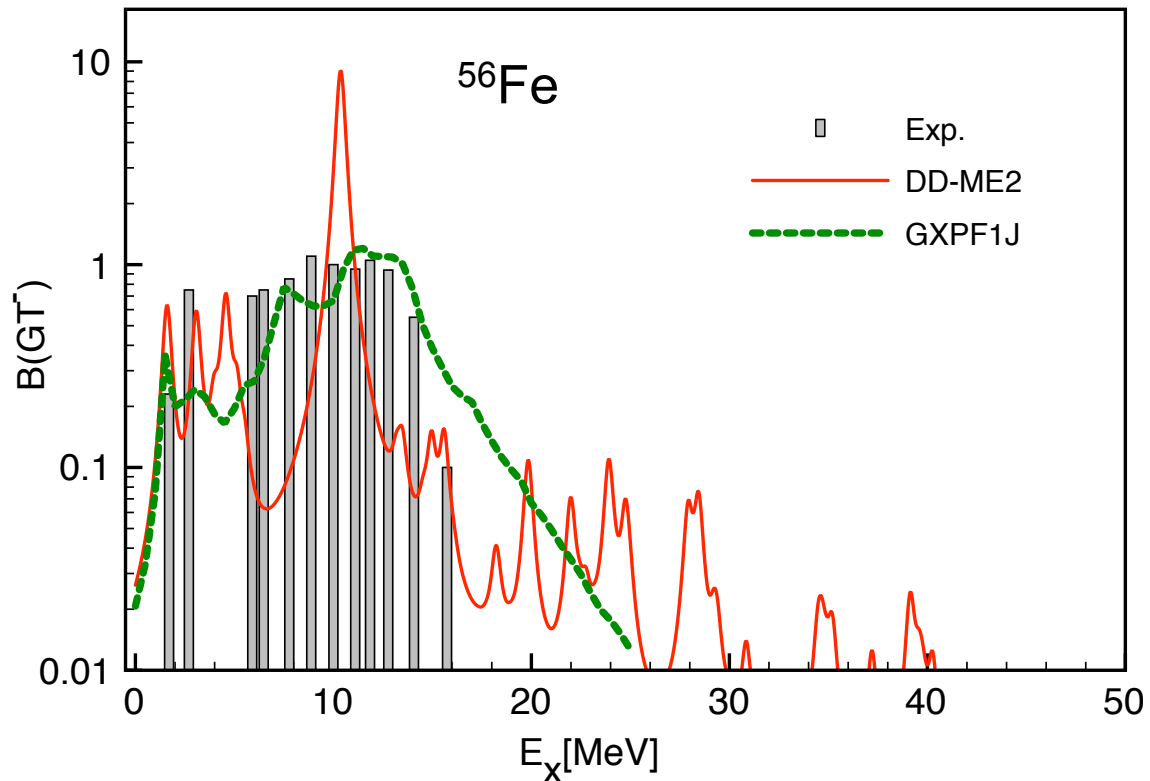
$S=0 \ T=1 \ J^\pi = 0^+$



SPIN-FLIP &
ISOSPIN-FLIP
EXCITATIONS

$S=1 \ T=1 \ J^\pi = 1^+$

GAMOW-TELLER TRANSITION STRENGTH FOR ^{56}Fe



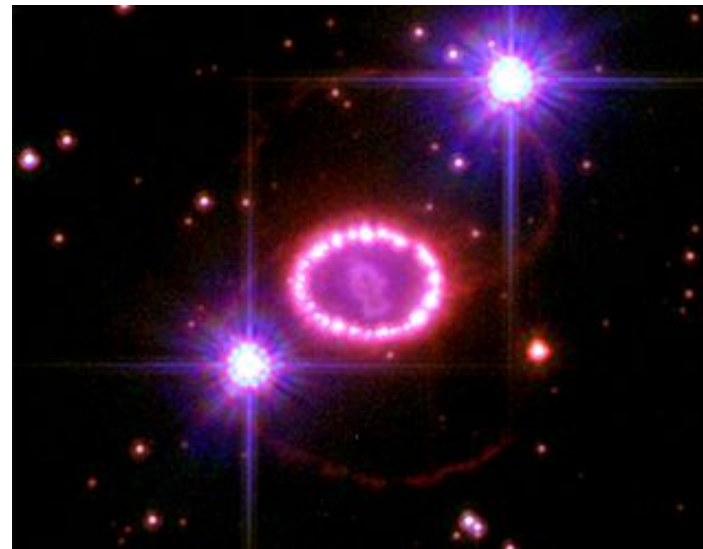
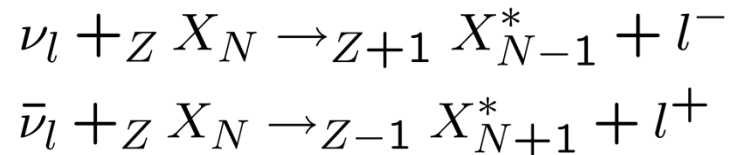
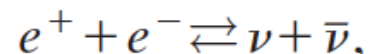
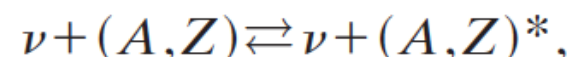
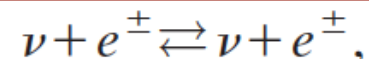
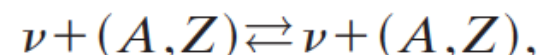
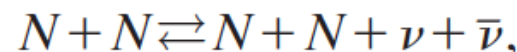
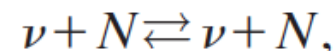
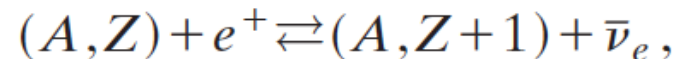
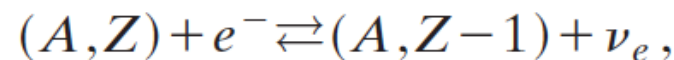
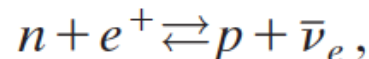
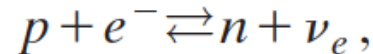
Gamow-Teller (GT) transitions calculated in two models:

- RQRPA (DD-ME2)
- Shell model (GXPF1J)
T. Suzuki et al.

- Shell model includes important correlations among nuclei, accurately reproduces the experimental GT strength. However, already in medium mass nuclei the model spaces become large, many nuclei and forbidden transitions remain beyond reach.
- RQRPA reproduces total GT strength and global properties of transition strength. It allows systematic calculations of high multipole excitations (forbidden transitions), possible extrapolations toward nuclei away from the valley of stability.

ASTROPHYSICALLY RELEVANT WEAK PROCESSES

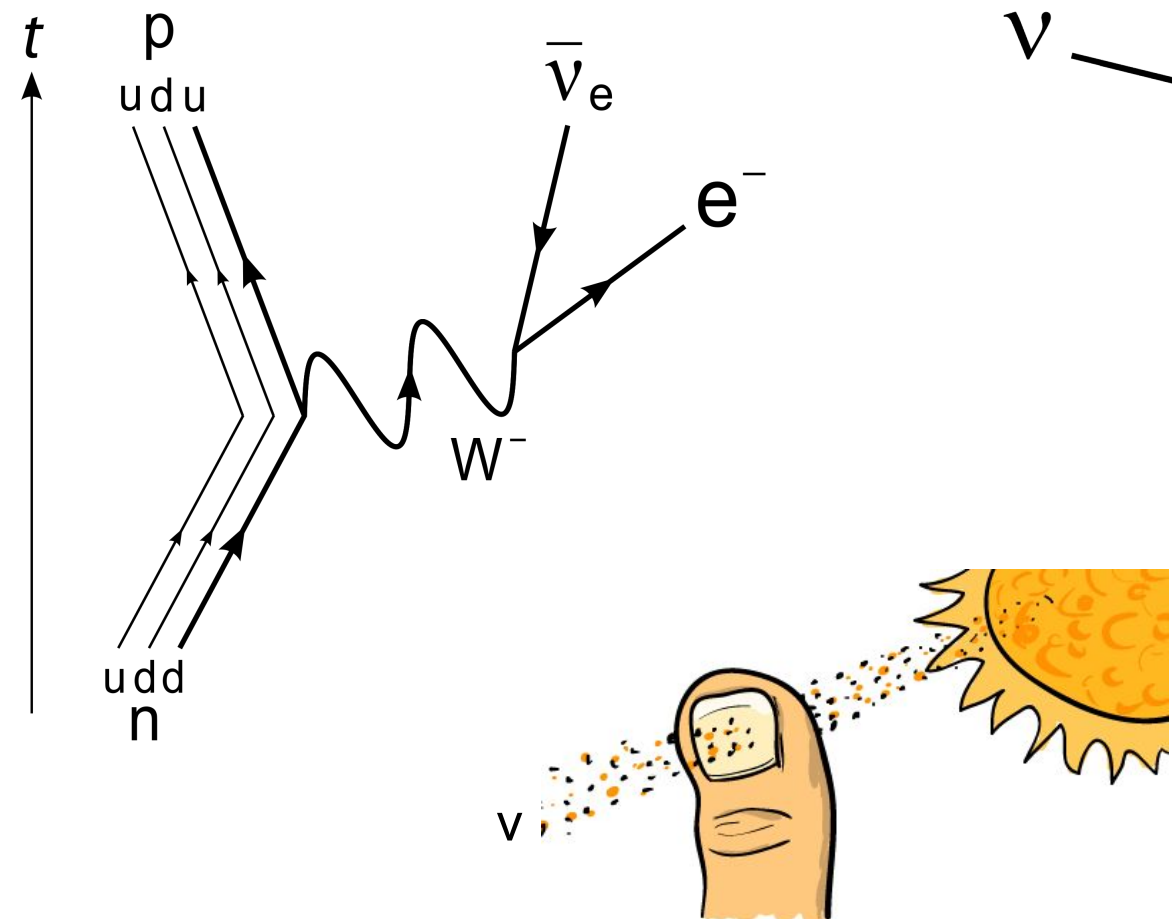
- Important weak processes during the star collapse and explosion:  [Kei Kotake](#)



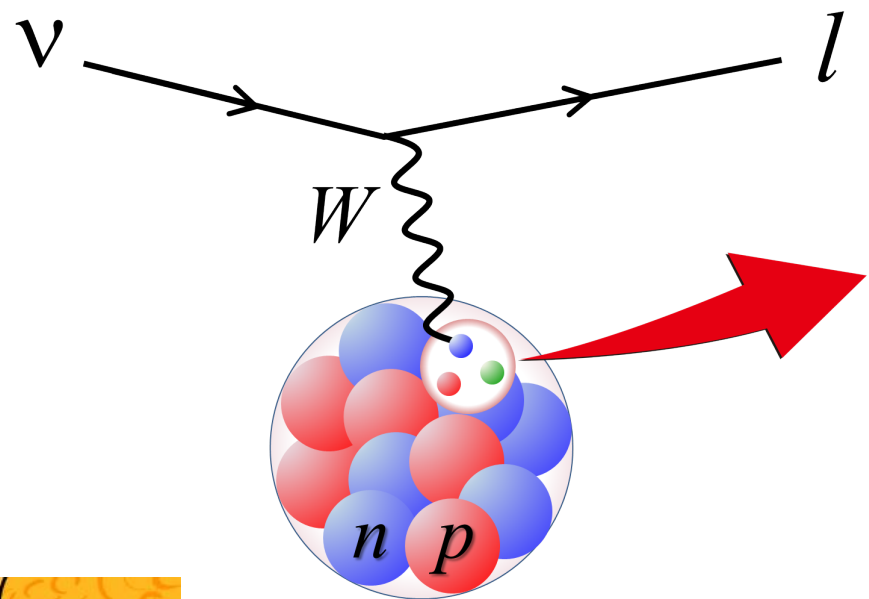
H. A. Bethe, Rev. Mod. Phys. 62 801 (1990)
 K. Langanke, G. Martinez-Pinedo Rev. Mod. Phys. 75, 819 (2003)

ASTROPHYSICALLY RELEVANT WEAK PROCESSES

β^- decay



Neutrino-nucleus reaction



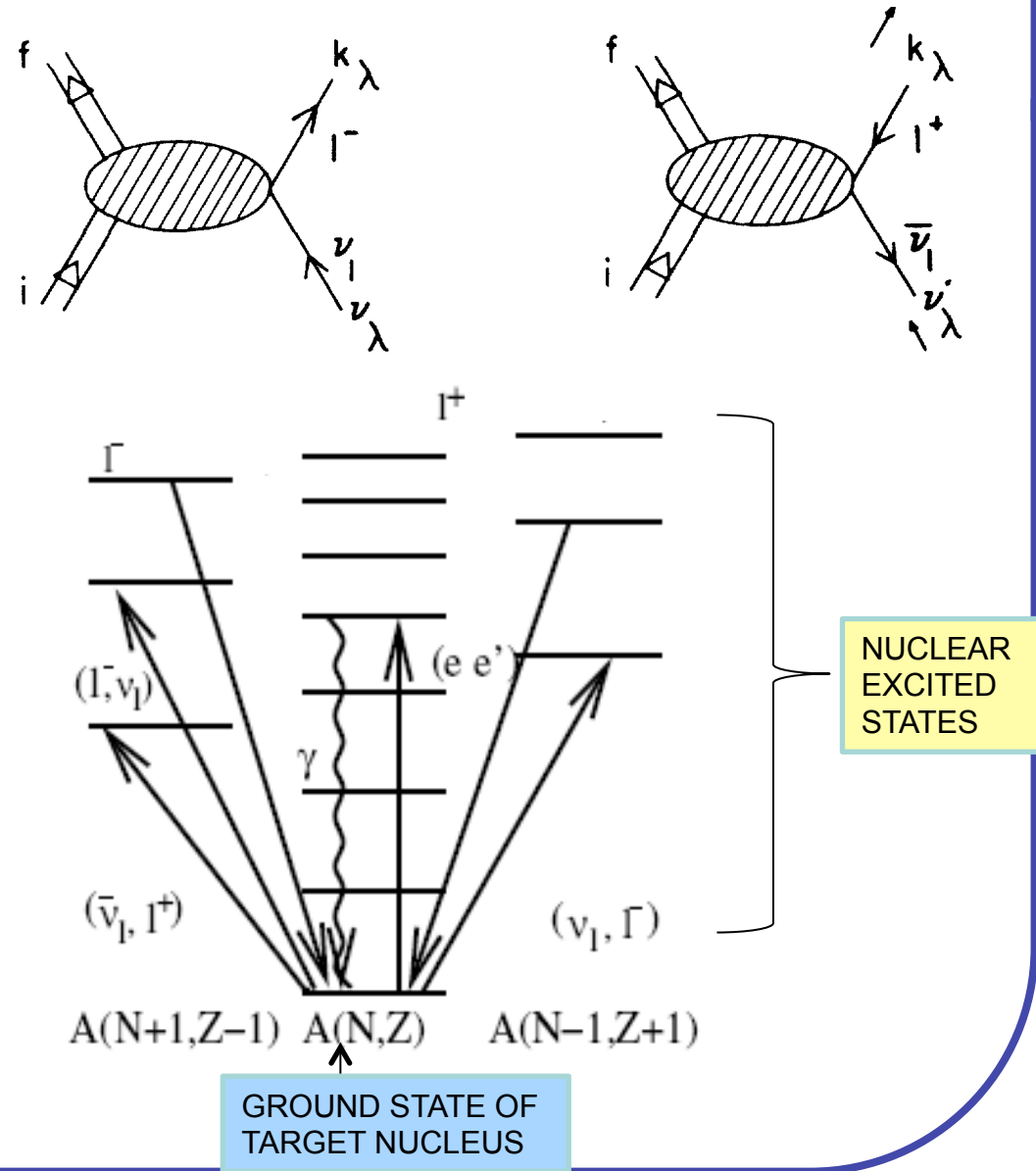
Why are all these processes weak?
→ Weak interaction!
 G_F - Fermi coupling constant

LOW-ENERGY NEUTRINO-NUCLEUS PROCESSES

Charged-current
neutrino-nucleus reactions

$$\nu_l + {}_Z X_N \rightarrow {}_{Z+1} X_{N-1}^* + l^-$$
$$\bar{\nu}_l + {}_Z X_N \rightarrow {}_{Z-1} X_{N+1}^* + l^+$$

The properties of nuclei and their excitations govern the neutrino-nucleus cross sections. Nuclear transitions induced by neutrinos involve operators with finite momentum transfer.



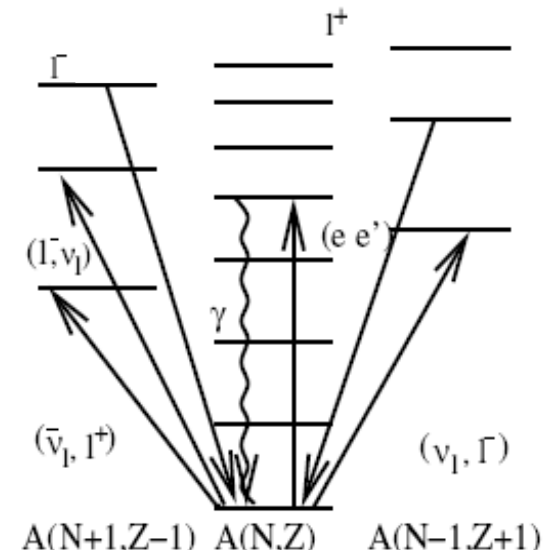
NEUTRINO-NUCLEUS CROSS SECTIONS

ν -nucleus cross sections

- Weak interaction Hamiltonian + EDF

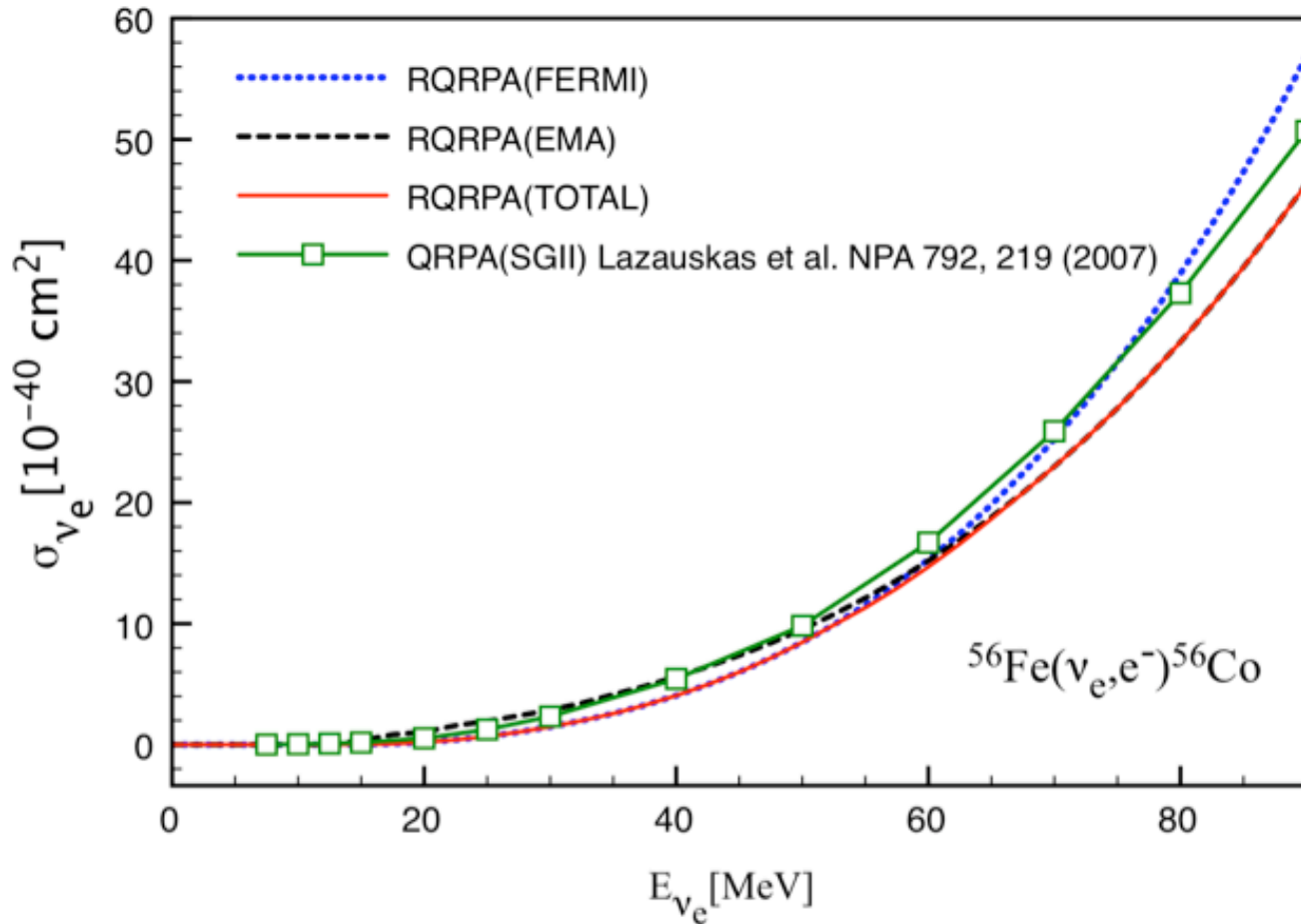
$$\hat{H}_W = -\frac{G}{\sqrt{2}} \int dx \mathcal{J}^\lambda(x) j_\lambda(x)$$

$$\begin{aligned} \frac{d\sigma_\nu}{d\Omega} &= \frac{2G_F^2 \cos^2 \theta_c}{\pi} \frac{E_l^2}{2J_i + 1} \\ &\times \left\{ \sum_{J \geq 1} \left\{ [1 - (\hat{\nu} \cdot \hat{q})(\hat{q} \cdot \beta)] \left[|\langle J_f | \hat{T}_J^{MAG} | J_i \rangle|^2 + |\langle J_f | \hat{T}_J^{EL} | J_i \rangle|^2 \right. \right. \right. \\ &\quad \left. \left. \left. + [\hat{q}(\hat{\nu} - \beta)] 2Re \langle J_f | \hat{T}_J^{MAG} | J_i \rangle \langle J_f | \hat{T}_J^{EL} | J_i \rangle^* \right] \right. \right. \\ &\quad \left. \left. + \sum_{J \geq 0} \left\{ (1 + \hat{\nu} \cdot \beta) |\langle J_f | \hat{\mathcal{M}}_J | J_i \rangle|^2 \right. \right. \right. \\ &\quad \left. \left. \left. + (1 - \hat{\nu} \cdot \beta + 2(\hat{\nu} \cdot \hat{q})(\hat{q} \cdot \beta)) |\langle J_f | \hat{\mathcal{L}}_J | J_i \rangle|^2 \right. \right. \\ &\quad \left. \left. \left. - [\hat{q}(\hat{\nu} + \beta)] 2Re \langle J_f | \hat{\mathcal{L}}_J | J_i \rangle \langle J_f | \hat{\mathcal{M}}_J | J_i \rangle^* \right\} \right] \right\} \end{aligned}$$



Transition matrix elements are described in a self-consistent way using relativistic Hartree-Bogoliubov model for the initial (ground) state and relativistic quasiparticle random phase approximation for excited states (RHB+RQRPA)

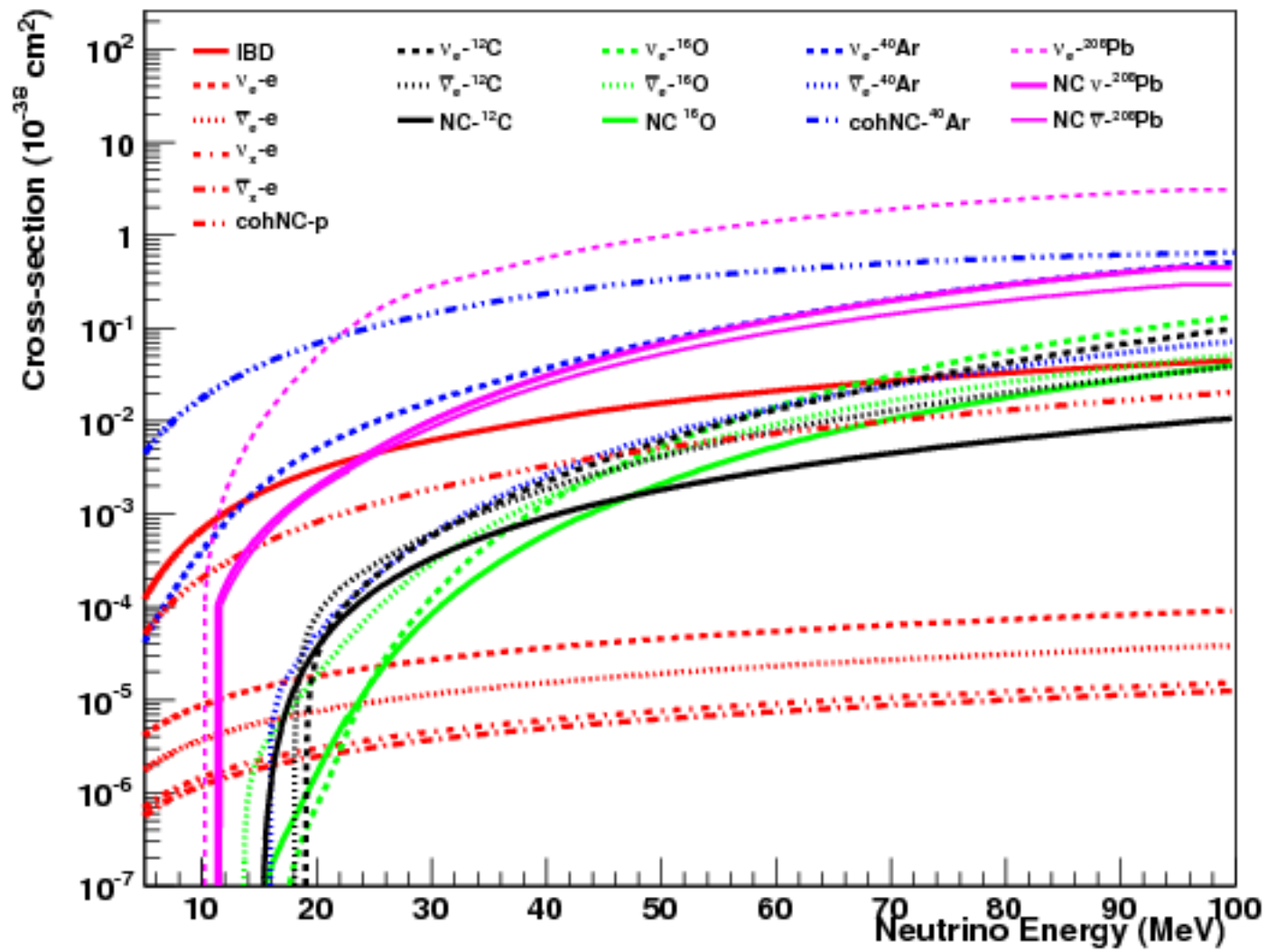
CHARGED-CURRENT NEUTRINO-NUCLEUS CROSS SECTIONS FOR ^{56}Fe



Model calculations include all multipoles (both parities) up to $J=5$. Coulomb interaction between outgoing electron and residual nucleus is taken into account.

Partly due to enhanced GT- transition strength, Skyrme functional results in larger cross sections than relativistic EDF.

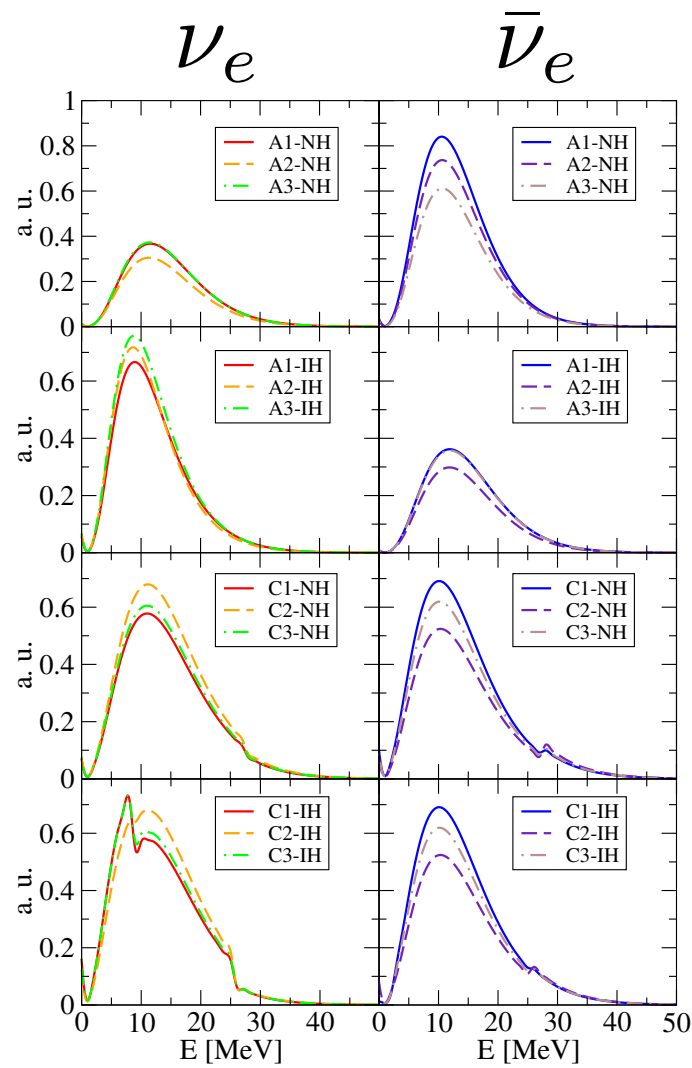
(ANTI)NEUTRINO INDUCED REACTION CROSS SECTIONS



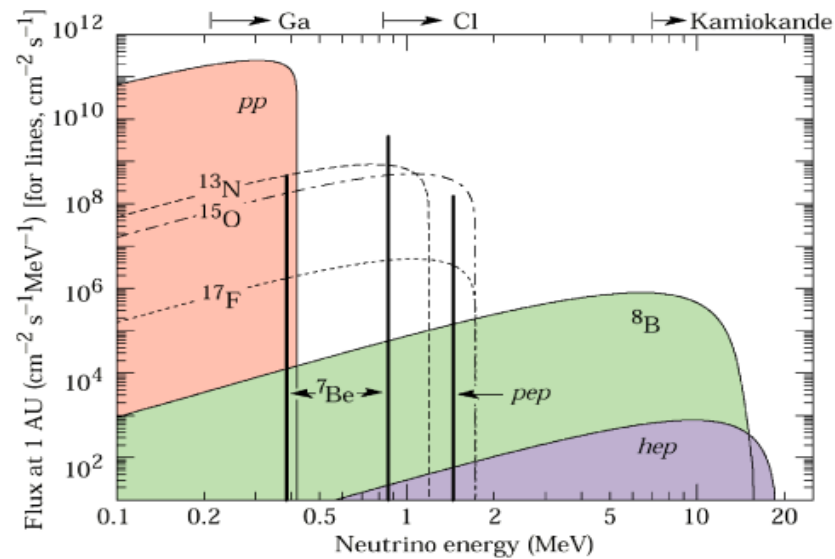
From: K. Scholberg

LOW-ENERGY NEUTRINO FLUXES

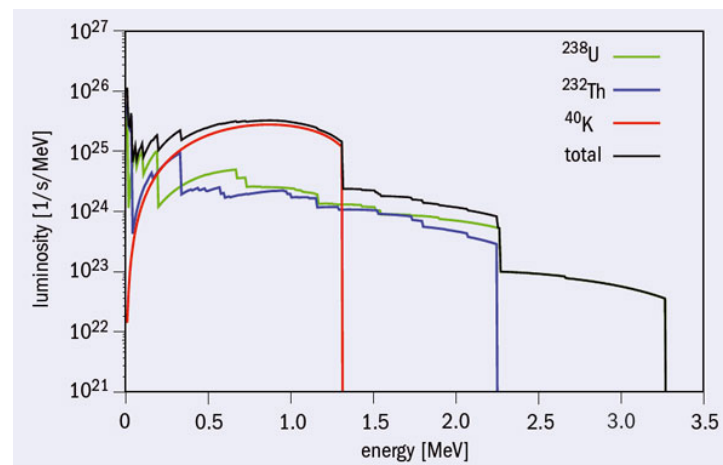
Supernova neutrinos



Solar neutrinos



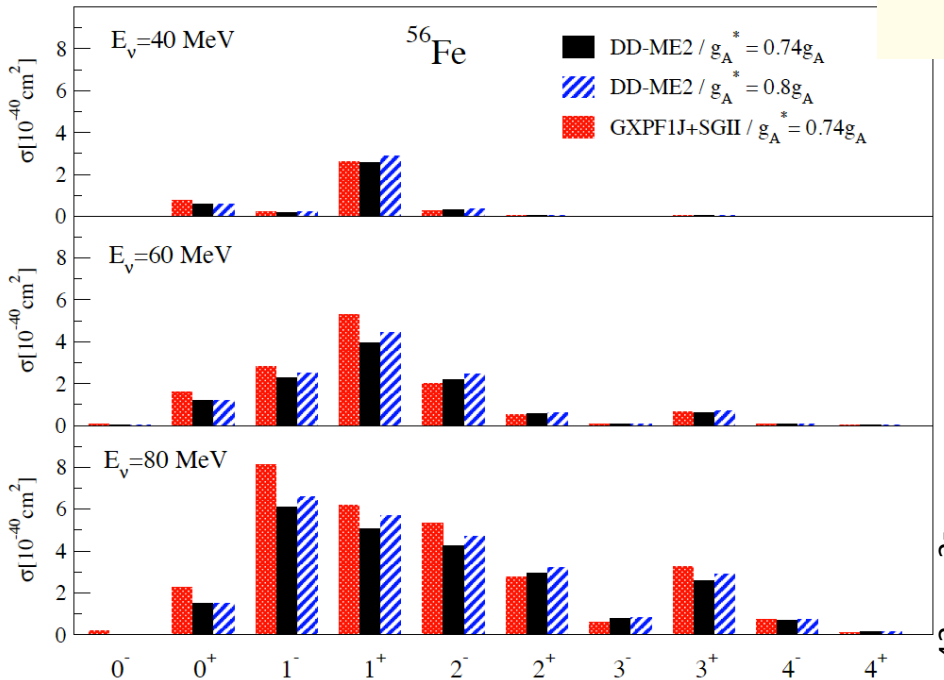
Geoneutrinos



D. Vale, T. Rauscher, N.P., JCAP02, 007 (2016)

T. Araki, et al., Nature 436, 499 (2005).

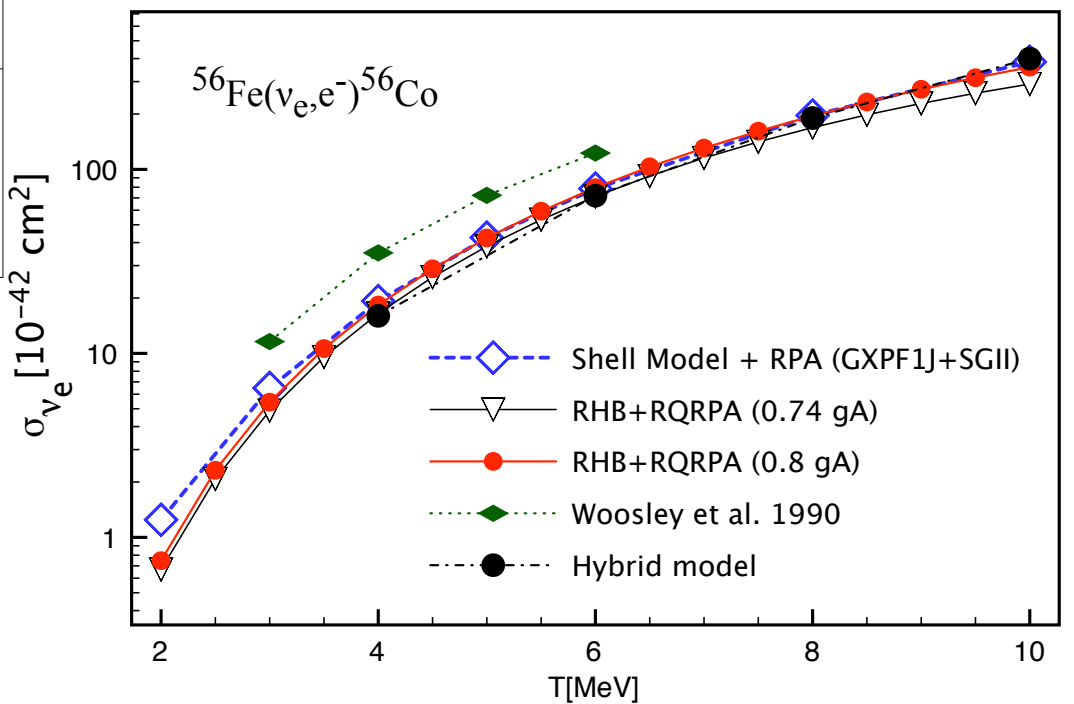
NEUTRINO-NUCLEUS CROSS SECTIONS



- The RNEDF allows systematic calculations of high multipole excitations (forbidden transitions), extrapolations toward nuclei away from the valley of stability.

- Multipole decomposition of the neutrino-nucleus cross sections: RNEDF (DD-ME2) vs. shell model + RPA (SGII) (T. Suzuki et al.)
 - Cross sections averaged over neutrino flux

$$\langle \sigma_\nu \rangle = \frac{\int dE_\nu \sigma_\nu(E_\nu) f(E_\nu)}{\int dE'_\nu f(E'_\nu)}$$

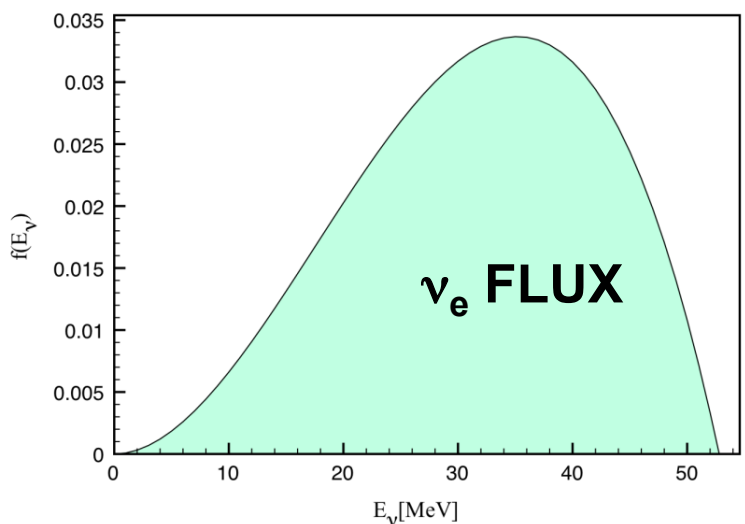


UNCERTAINTIES IN MODELING ν -NUCLEUS CROSS SECTIONS

- Neutrino-nucleus cross sections for ^{56}Fe target, averaged over the electron neutrino from μ^+ decay at rest (DAR)

$^{56}\text{Fe}(\nu_e, e^-) ^{56}\text{Co}$	$\langle \sigma \rangle (10^{-42}\text{cm}^2)$
QRPA(SIII) (Lazauskas et al.)	352
Shell model (GXPF1J) + RPA (SGII) (T. Suzuki et al.)	259
RPA (Kolbe, Langanke)	240
QRPA (Cheoun et al.)	173
PN-RQRPA	263
EXP. (KARMEN)	$256 \pm 108 \pm 43$

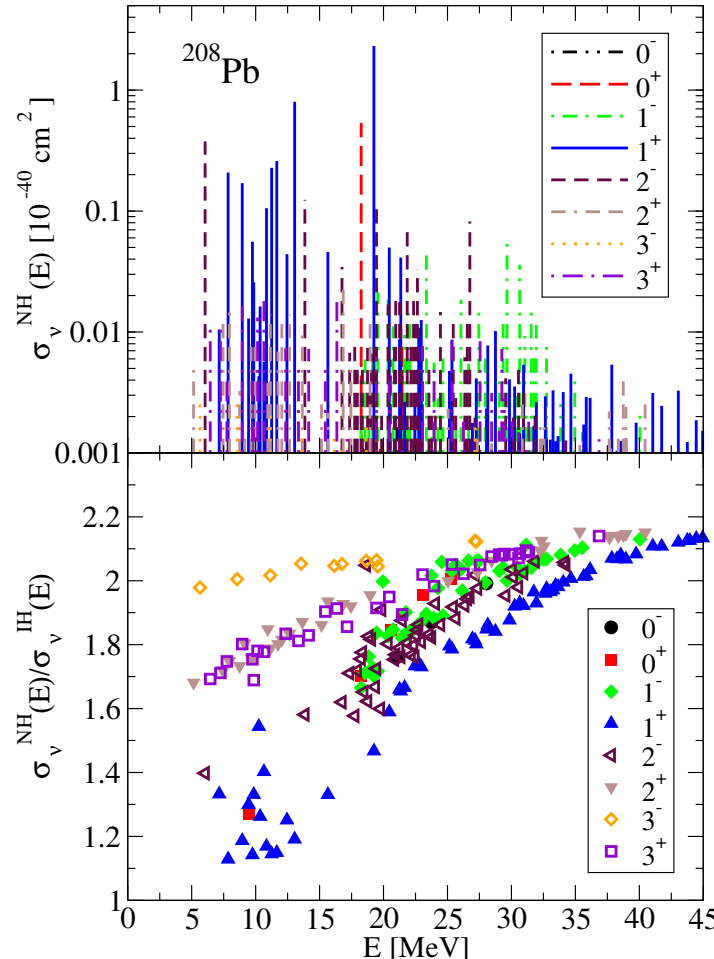
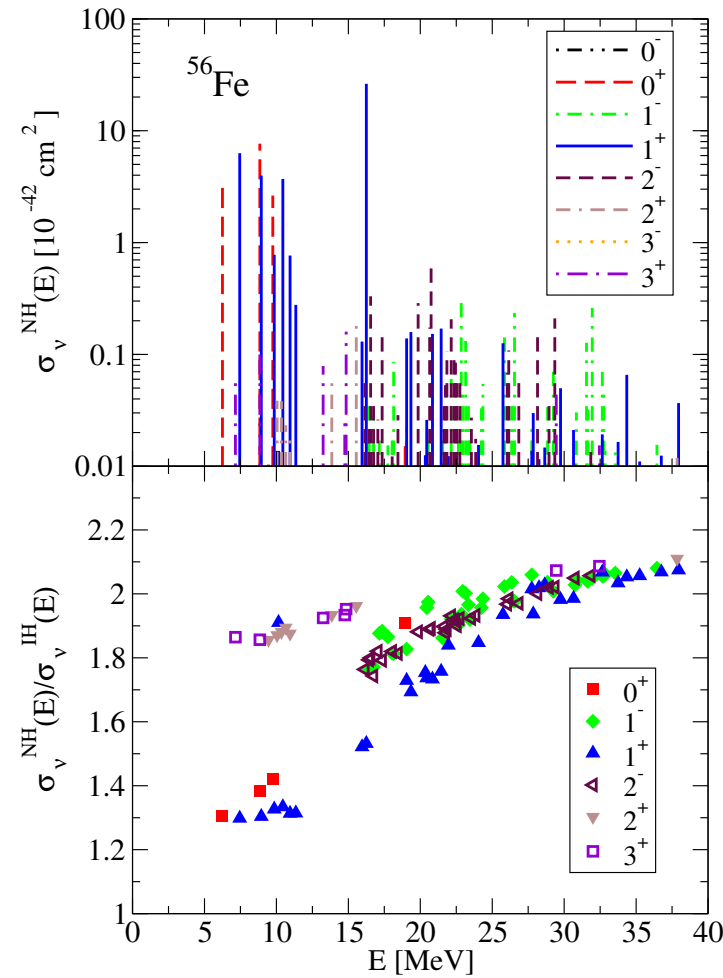
$$\langle \sigma_\nu \rangle = \frac{\int dE_\nu \sigma_\nu(E_\nu) f(E_\nu)}{\int dE'_\nu f(E'_\nu)}$$



$$\langle \sigma \rangle_{th} = (258 \pm 57) \times 10^{-42} \text{cm}^2$$

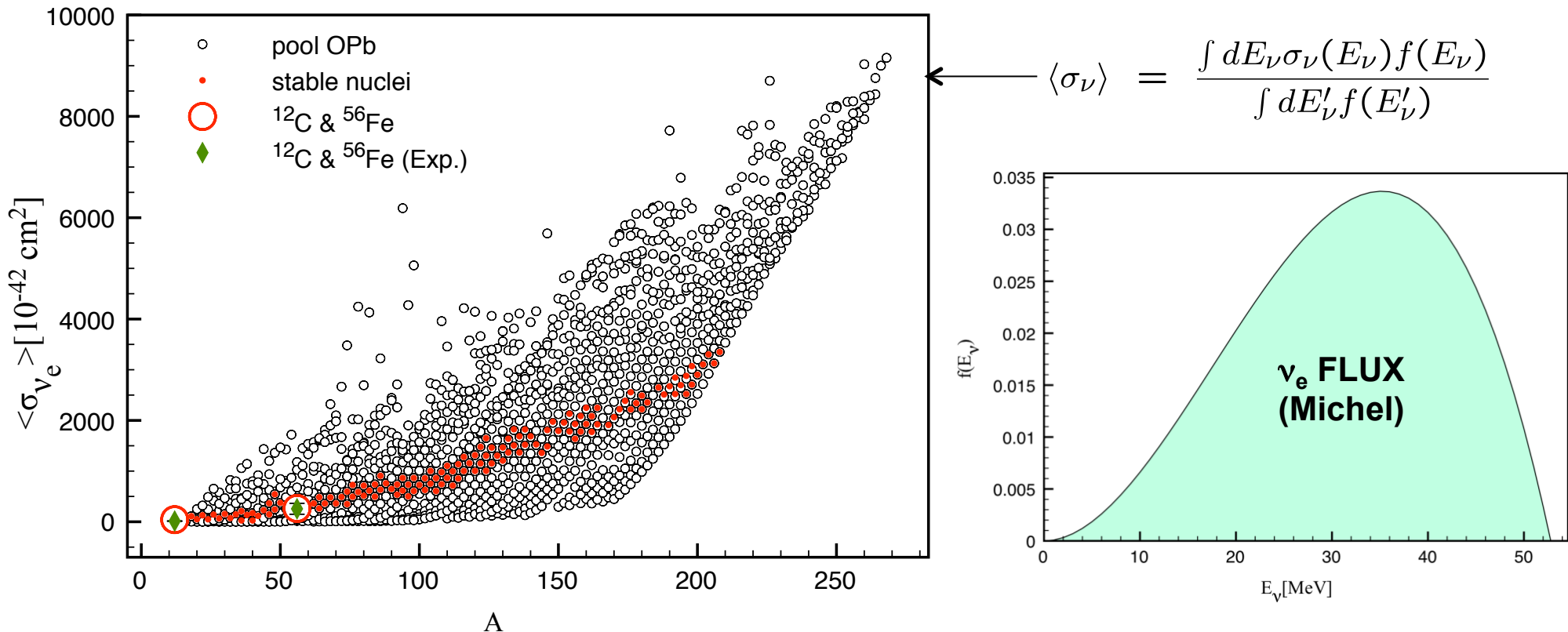
NEUTRINO-NUCLEUS CROSS SECTIONS

- neutrino-nucleus cross sections for the incoming neutrinos from supernova cooling phase



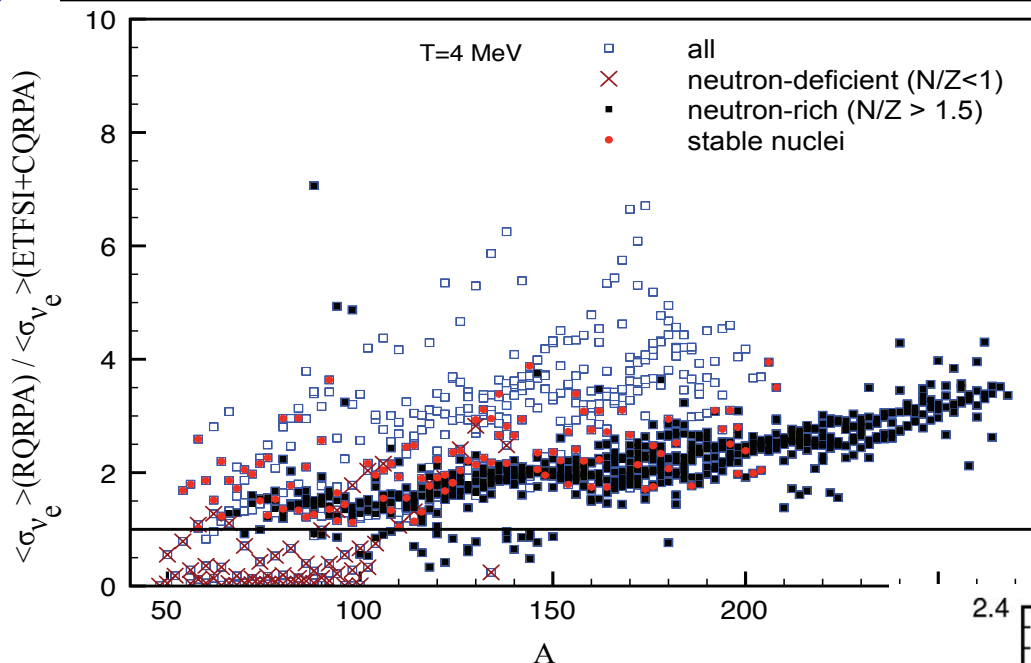
LARGE-SCALE CALCULATIONS OF ν_e -NUCLEUS CROSS SECTIONS

- The cross sections averaged over the neutrino spectrum from muon DAR.



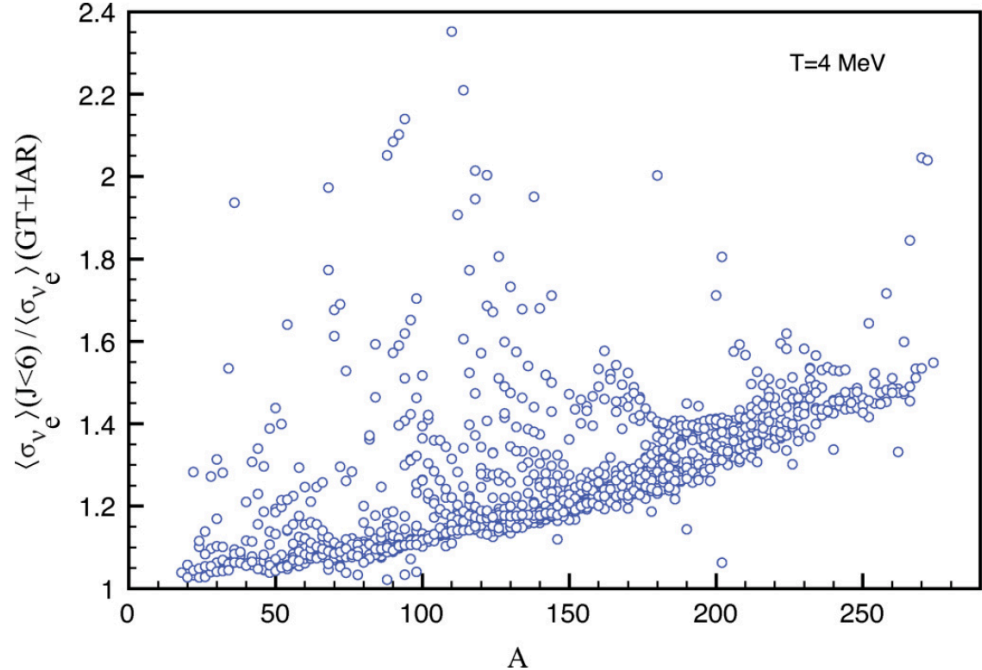
- Exp. data available only for ^{12}C and ^{56}Fe
- The cross sections become considerably enhanced in neutron-rich nuclei, while those in neutron-deficient and proton-rich nuclei are small (blocking).

LARGE-SCALE CALCULATIONS OF ν -NUCLEUS CROSS SECTIONS



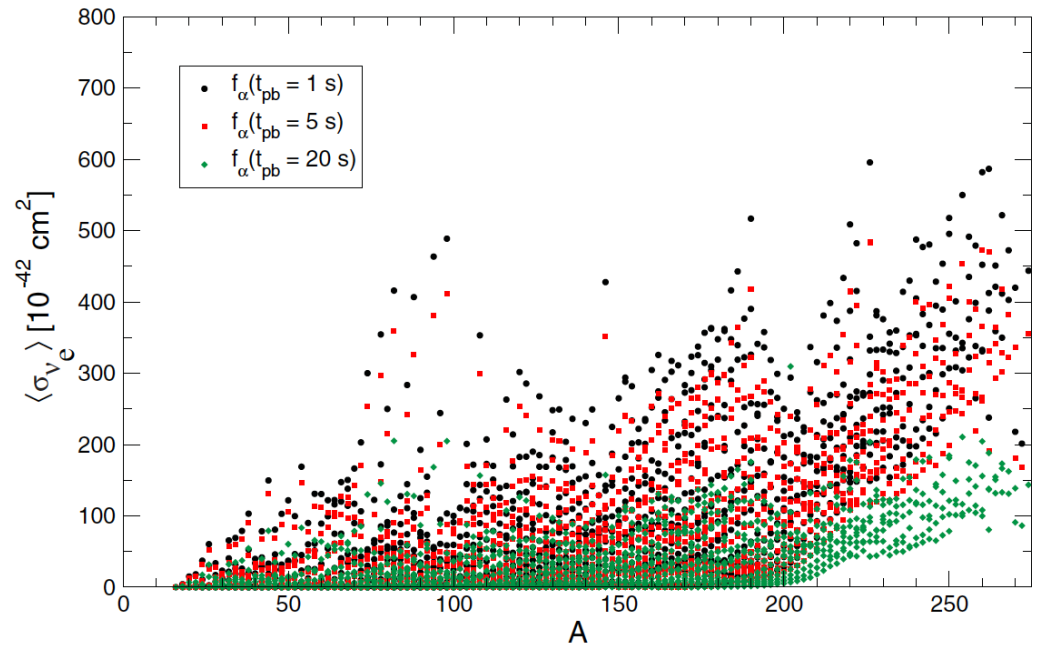
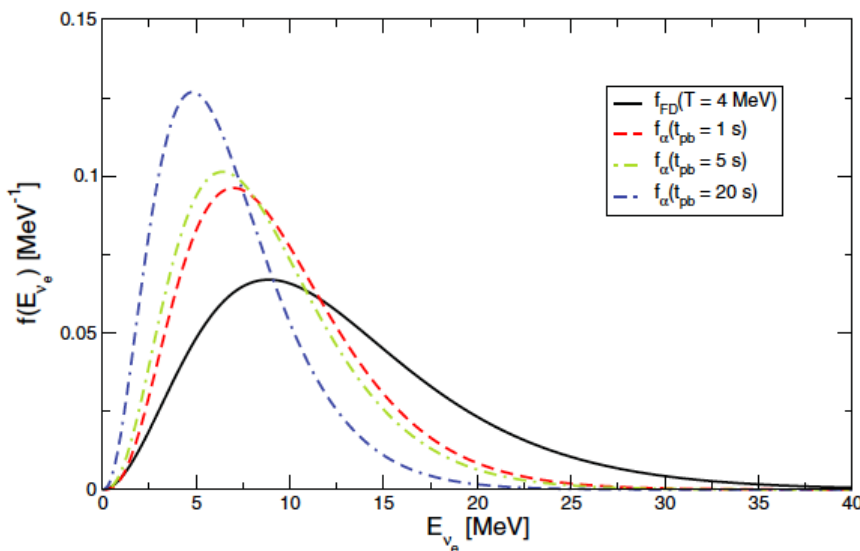
- The ν -nucleus cross sections averaged over the Fermi-Dirac distribution ($T=4$ MeV)
- Comparison of the RNEDF results with the ETFSI+CQRPA (only IAS & GT transitions;
I. N. Borzov and S. Goriely, Phys. Rev. C 62, 035501 (2000).)

Contributions of higher multipoles can be significant, esp. for heavy nuclei.

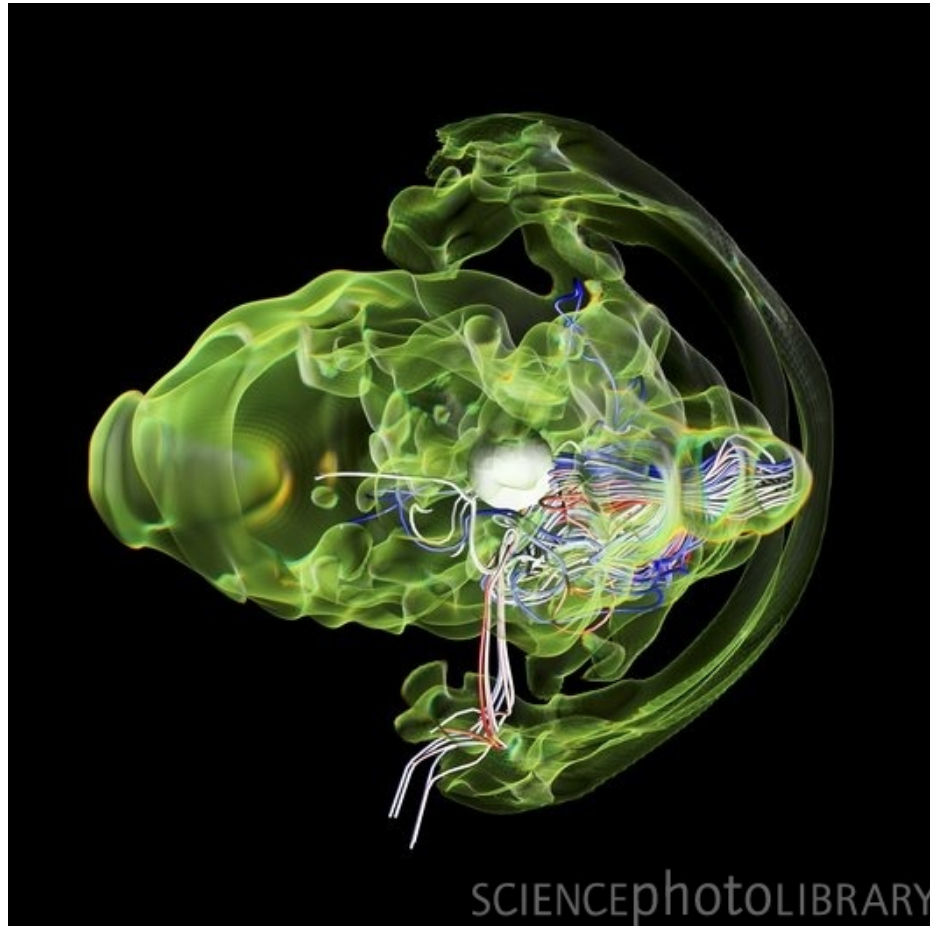


LARGE-SCALE CALCULATIONS OF ν -NUCLEUS CROSS SECTIONS

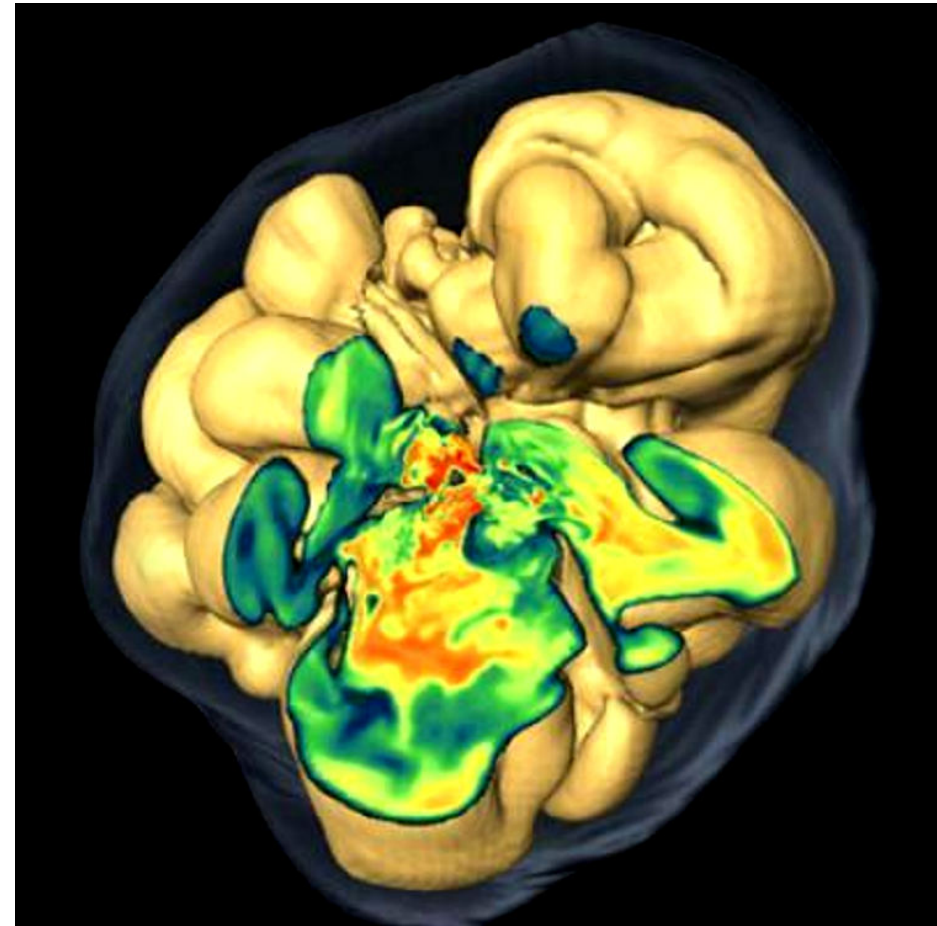
- Neutrino-nucleus cross sections for neutrinos from core collapse supernova simulation
- Supernova model based on general relativistic radiation hydrodynamics and three flavor Boltzmann neutrino transport (Fe core progenitor; 18 M_{solar}) (**T. Fischer**)
- Simulations show continuous decreasing of neutrino luminosities and average energies after the supernova explosion is launched (deleptonization of central protoneutron star)
- Neutrino fluxes and flux-averaged cross sections using neutrino spectra at different postbounce times $t_{pb} = 1\text{ s}, 5\text{ s}, 20\text{ s}$:



HOW SUPERNOVA CORE COLLAPSE WORK?



T. Mezzacappa et al., ORNL, GenASiS code (2009)



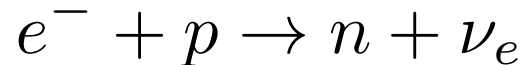
N. J. Hammer, H.-Th. Janka and E. Müller
Astrophys. J. 714, 1371 (2010)

STELLAR ELECTRON CAPTURE

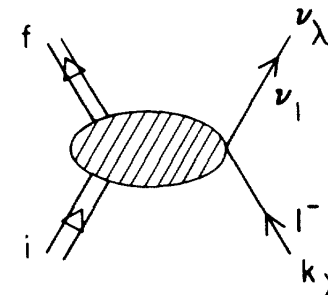
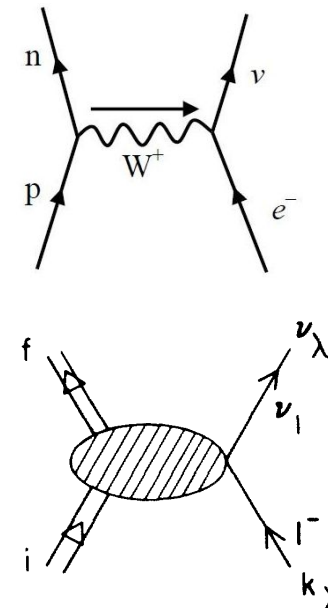
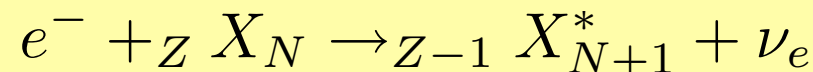
- The core of a massive star at the end of hydrostatic burning is stabilized by electron degeneracy pressure (as long as its mass does not exceed the Chandrasekhar limit)
- Electron capture reduces the number of electrons available for pressure support (in opposition to nuclear beta decay)

Kei Kotake

Electron capture on protons



Electron capture on nuclei



- Electron capture on iron-group nuclei initiates the gravitational collapse of the core of a massive star, triggering a supernova explosion

STELLAR ELECTRON CAPTURE

- Initial supernova shock location and strength depend on amount of electron capture on nuclei (and protons) during stellar core collapse
- In the early stage of the collapse $\rho \leq 10^{10} g cm^{-3}$ electron chemical potential is of the order of the nuclear Q value, electron captures are sensitive to the details of Gamow-Teller GT⁺ strength;

$$T \approx 0.3 - 0.8 MeV$$

$$A < 65$$

Electron capture also occurs for higher densities and temperatures

→ total GT strength and centroid are relevant,

at $\rho \geq 10^{11} g cm^{-3}$ forbidden transitions should also be taken into account;

$$T \approx 1 MeV$$

$$A \geq 65$$

- Shell model, Random Phase Approximation (RPA), QRPA, Hybrid model

K. Langanke et al., Phys. Rev. Lett. 90, 241102 (2003)

A.A. Dzhioev et al., Phys. Rev. C 81, 015804 (2010)

A. Juodagalvis et al., Nucl. Phys. A 848, 454 (2010)

SELF-CONSISTENT THEORY OF ELECTRON CAPTURE

- EDF methods in modeling electron capture in supernova core collapse
- Stellar electron capture: nuclear transition matrix elements are determined by fully self-consistent theory:

a) Hartree-Fock+RPA (Skyrme functionals)

- N. P., G. Colò, E. Khan, and D. Vretenar, Phys. Rev. C 80, 055801 (2009)

b) Relativistic mean field + relativistic RPA (DD-ME2)

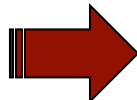
- Y. F. Niu, N. P., D. Vretenar, and J. Meng, Phys. Lett. B 681, 315 (2009)
- N. P., J. Phys. G: Nucl. Part. Phys. 37, 064014 (2010)

Finite temperature effects are described by Fermi-Dirac occupation factors for each single-nucleon state at the level of HF (or RMF), the same occupation factors are transferred to RPA

FINITE TEMPERATURE RANDOM PHASE APPROXIMATION (FTRPA)



The initial state of nucleus is described by the finite temperature RMF/HF



Due to finite temperature, some particle states become partially occupied, some hole states too

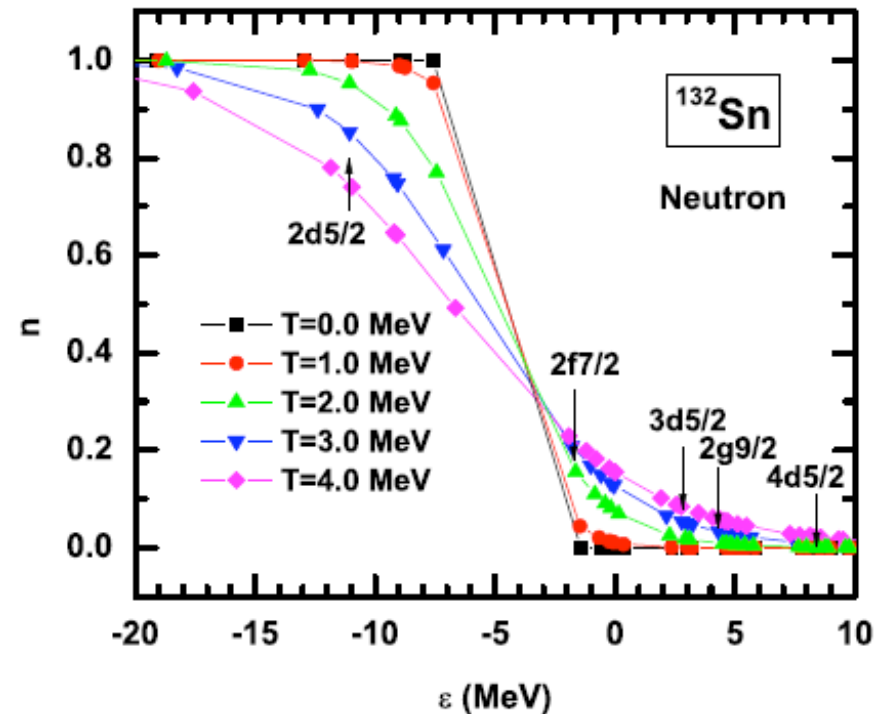
Equation of motion:

$$i\partial_t \hat{\rho} = [\hat{h}[\hat{\rho}] + \hat{f}(t), \hat{\rho}]$$

$$\hat{\rho}(t) = \hat{\rho}^0 + \delta\hat{\rho}(t)$$

$$\rho_{kl}^0 = \delta_{kl} n_k = \begin{cases} [1 + \exp(\frac{\epsilon_i - \mu}{kT})]^{-1} & \text{for states in the Fermi sea} \\ 0 & \text{for unoccupied states in the Dirac sea} \end{cases}$$

$$\begin{pmatrix} A & B \\ -B^* & -A^* \end{pmatrix} \begin{pmatrix} X \\ Y \end{pmatrix} = \hbar\omega \begin{pmatrix} X \\ Y \end{pmatrix}$$



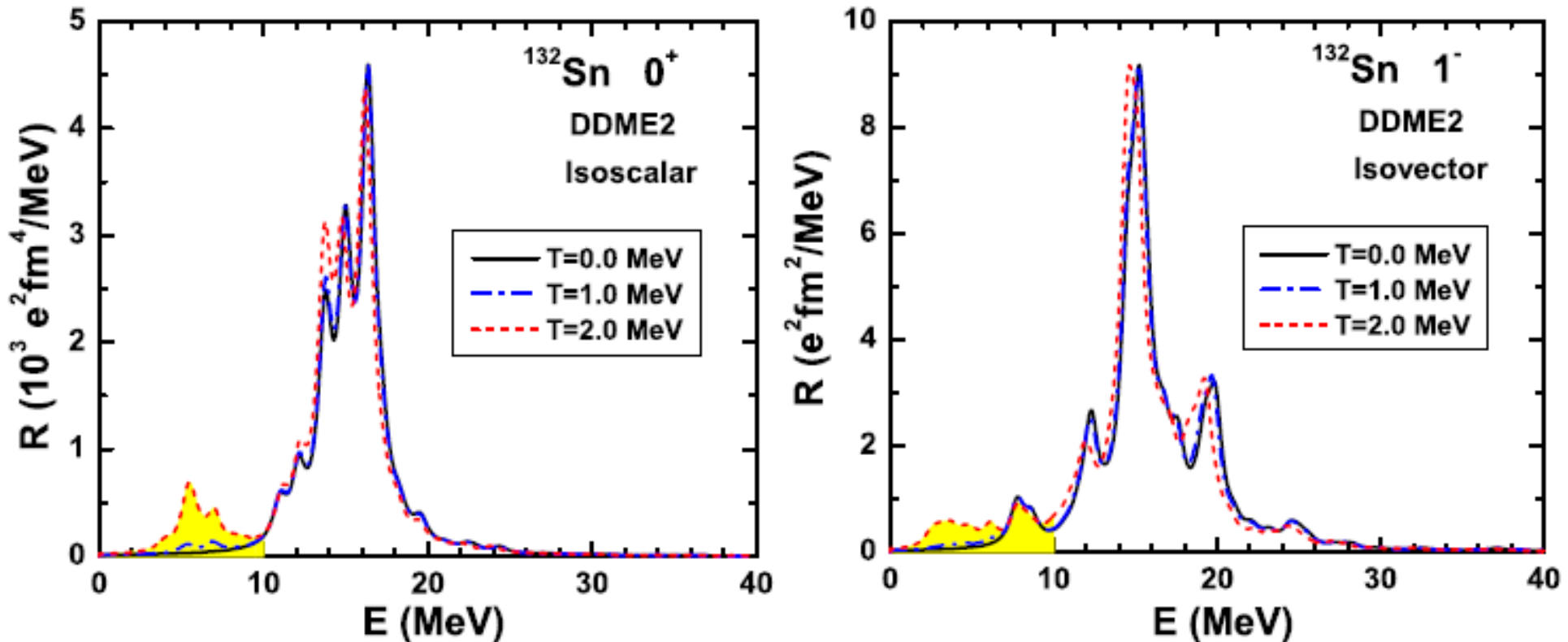
Small-amplitude limit

- for states in the Fermi sea
- for unoccupied states in the Dirac sea

FTRPA

MONOPOLE AND DIPOLE RESPONSE AT FINITE TEMPERATURE

What is the structure of low-energy excitations at finite temperature?



Since at finite temperature new transition channels become open, the Pygmy dipole strength becomes distributed toward lower energies, but its main peaks remain their structure

ELECTRON CAPTURE CROSS SECTIONS

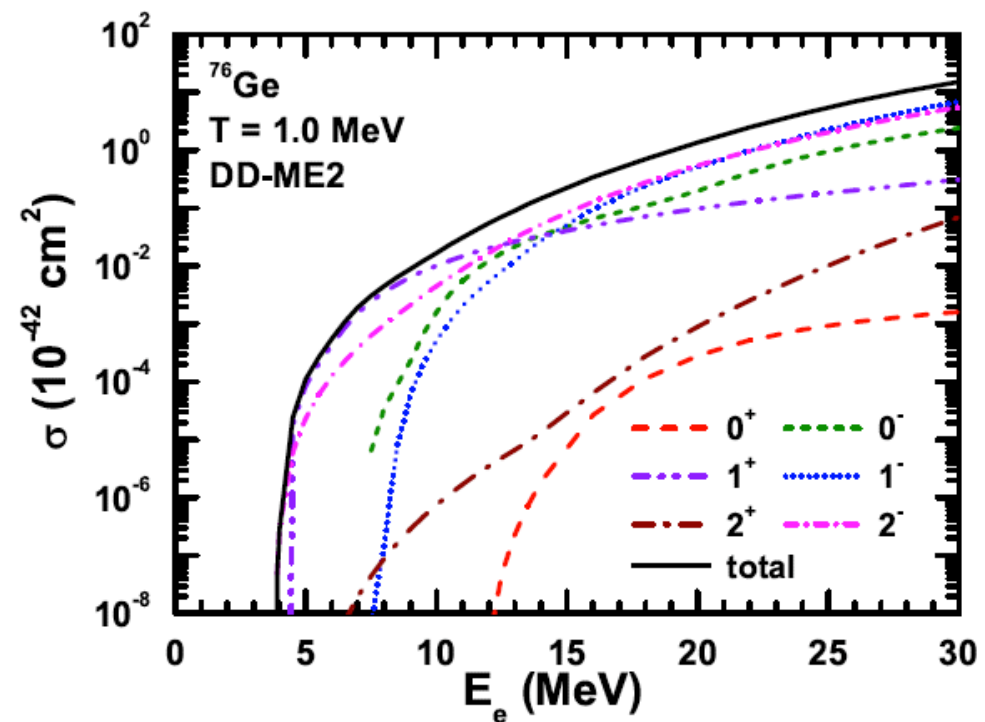
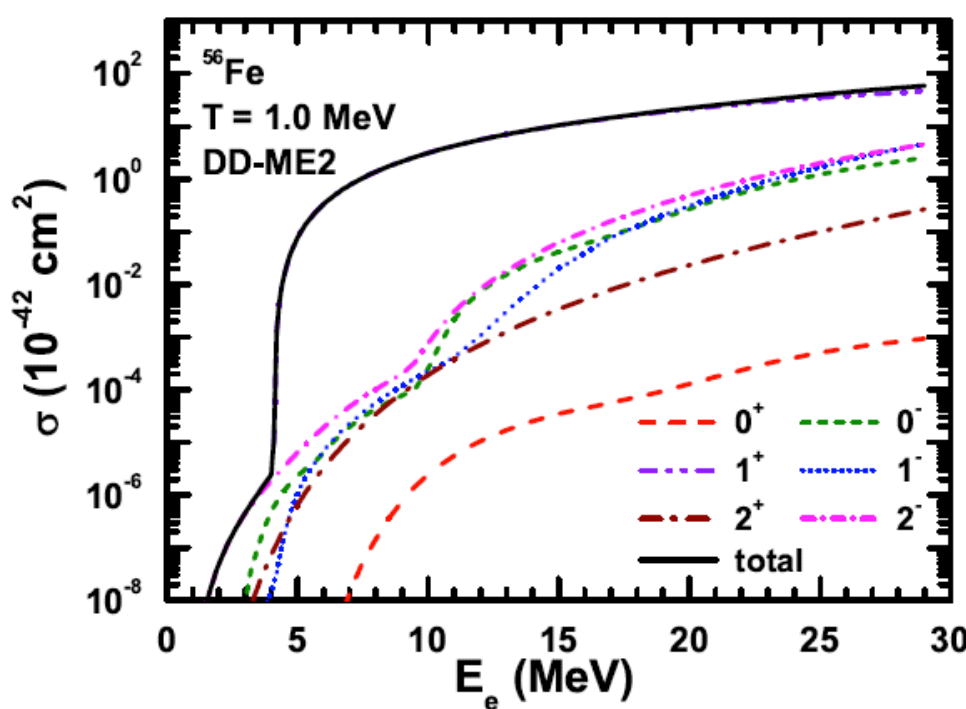
Cross section is derived from the Fermi's golden rule, assuming weak Hamiltonian in current-current form

Transition matrix elements include charge ($\hat{\mathcal{M}}_J$) , longitudinal ($\hat{\mathcal{L}}_J$), transverse electric (\hat{T}_J^{EL})and transverse magnetic (\hat{T}_J^{MAG}) multipole operators

$$\frac{d\sigma}{d\Omega} = \frac{G_F^2 \cos^2 \theta_c}{2\pi} \frac{F(Z, E_e)}{(2J_i + 1)} \times \left\{ \sum_{J \geq 1} \frac{E_\nu^2}{(1 + E_\nu/M_T)} \left\{ (1 - (\hat{\nu} \cdot \hat{q})(\beta \cdot \hat{q})) \left[|\langle J_f | \hat{T}_J^{MAG} | J_i \rangle|^2 + |\langle J_f | \hat{T}_J^{EL} | J_i \rangle|^2 \right] \right. \right. \\ - 2\hat{q} \cdot (\hat{\nu} - \beta) \text{Re} \langle J_f | \hat{T}_J^{MAG} | J_i \rangle \langle J_f | \hat{T}_J^{EL} | J_i \rangle^* \Big\} \\ + \sum_{J \geq 0} \frac{E_\nu^2}{(1 + E_\nu/M_T)} \left\{ (1 - \hat{\nu} \cdot \beta + 2(\hat{\nu} \cdot \hat{q})(\beta \cdot \hat{q}) \langle J_f | \hat{\mathcal{L}}_J | J_i \rangle)^2 + (1 + \hat{\nu} \cdot \beta) \langle J_f | \hat{\mathcal{M}}_J | J_i \rangle^2 \right. \\ \left. \left. - 2\hat{q}(\hat{\nu} + \beta) \text{Re} \langle J_f | \hat{\mathcal{L}}_J | J_i \rangle \langle J_f | \hat{\mathcal{M}}_J | J_i \rangle^* \right\} \right\}$$

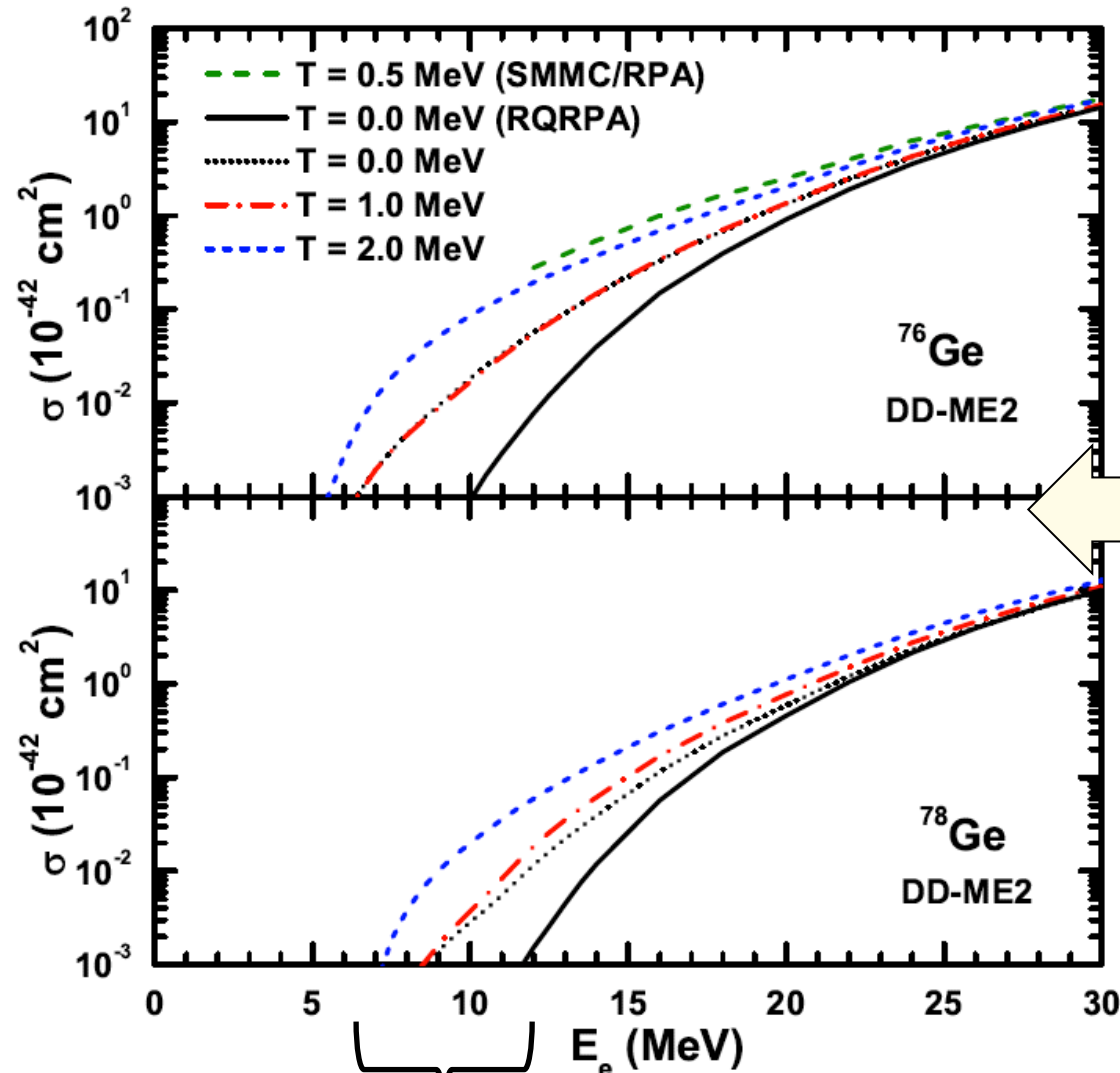
ELECTRON CAPTURE (EC) CROSS SECTIONS

How various multipole transitions contribute to the EC cross sections?



For ^{56}Fe the electron capture is dominated by the GT+ transitions, while for neutron-rich nuclei (^{76}Ge) forbidden transitions play more prominent role)

STELLAR ELECTRON CAPTURE ON NEUTRON RICH Ge ISOTOPES

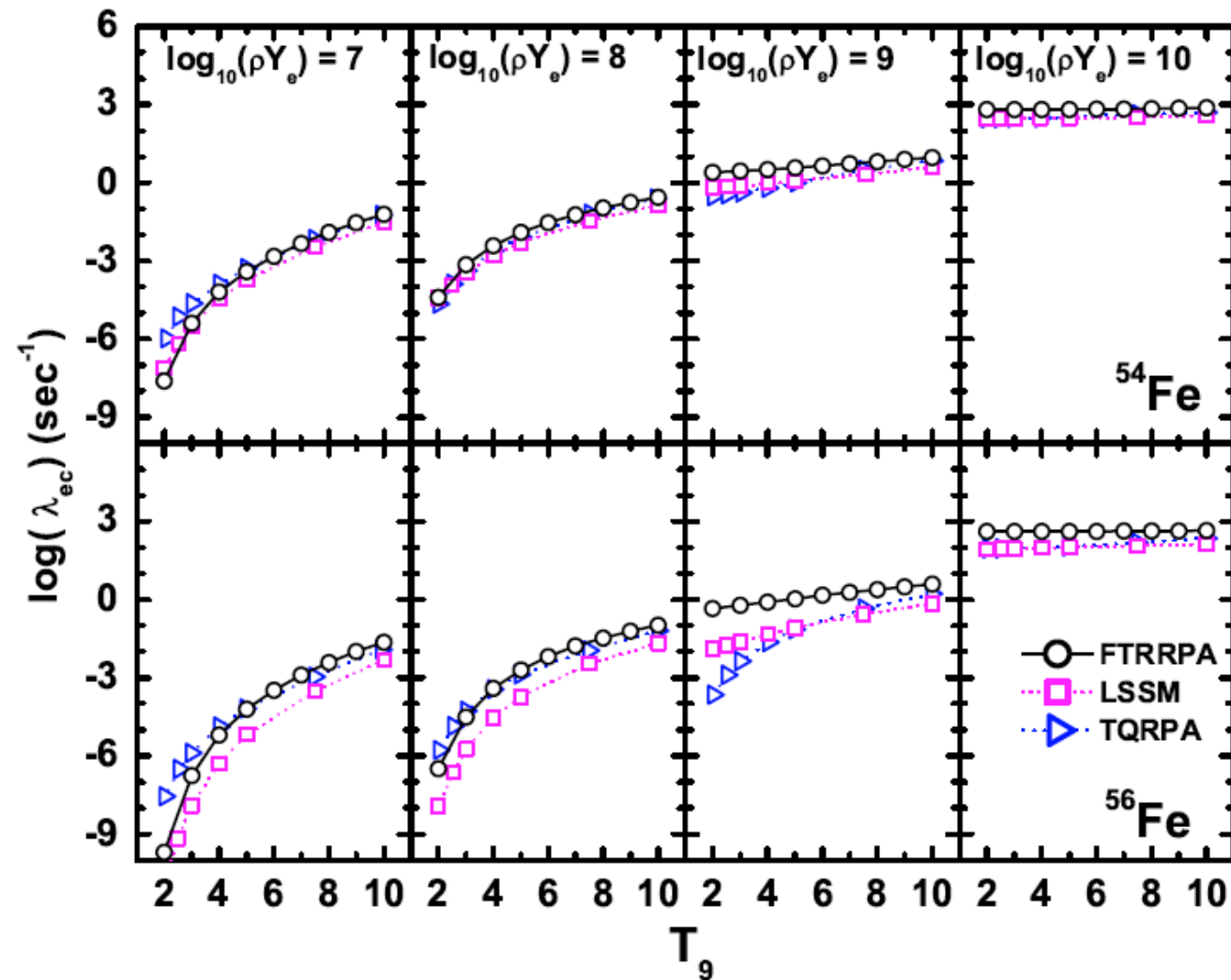


DEPENDENCE OF THE
ELECTRON CAPTURE
CROSS SECTIONS ON
TEMPERATURE

Unblocking effect: electron-capture threshold energy decreases with temperature.

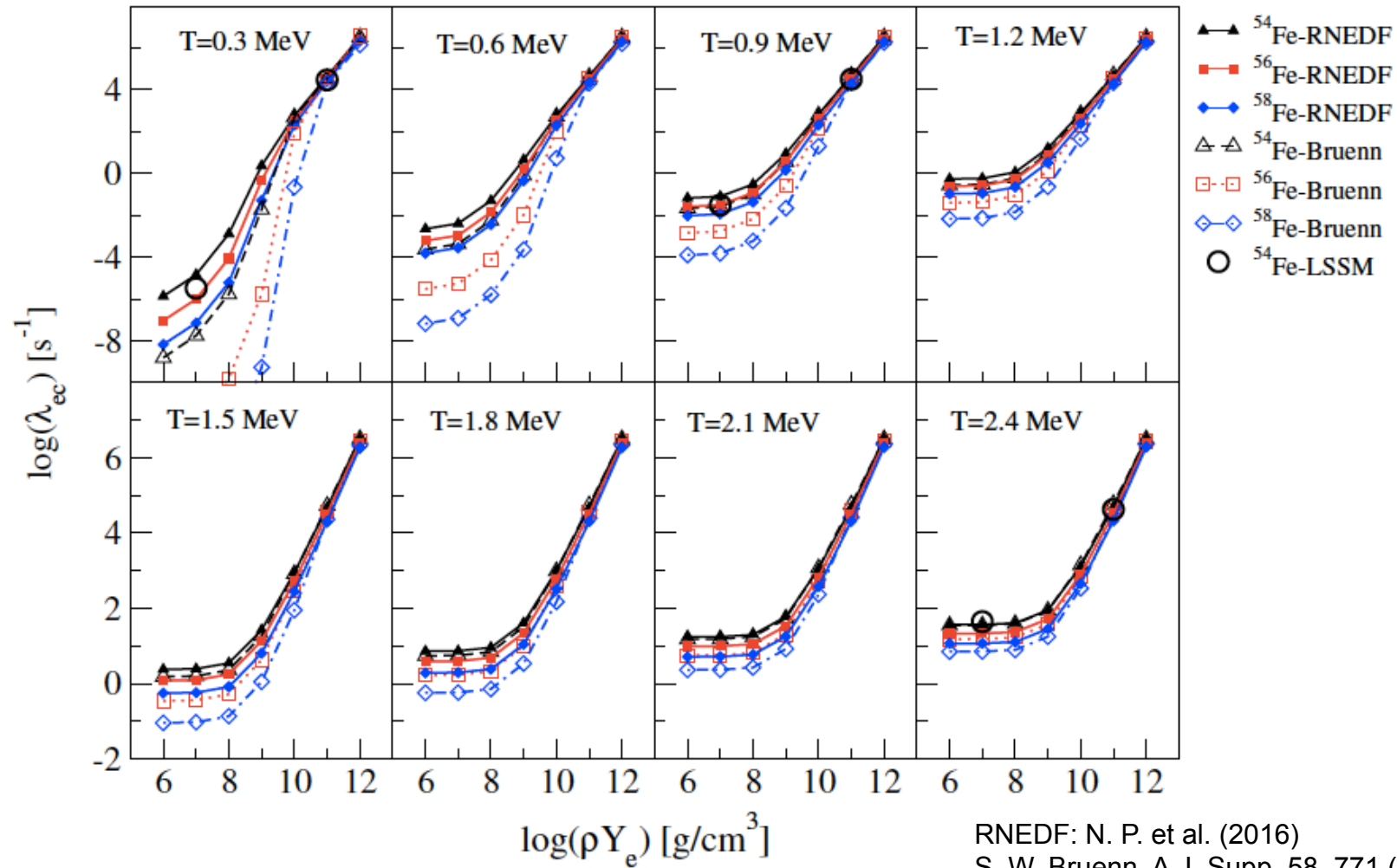
STELLAR ELECTRON CAPTURE RATES ON Fe ISOTOPES

$$\lambda_{\text{ec}} = \frac{1}{\pi^2 \hbar^3} \int_{E_e^0}^{\infty} p_e E_e \sigma_{\text{ec}}(E_e) f(E_e, \mu_e, T) dE_e$$



STELLAR ELECTRON CAPTURE RATES ON Fe ISOTOPES

- Comparison between the RNEDF rates and the Bruenn rates



STELLAR ELECTRON CAPTURE RATES ON Fe ISOTOPES

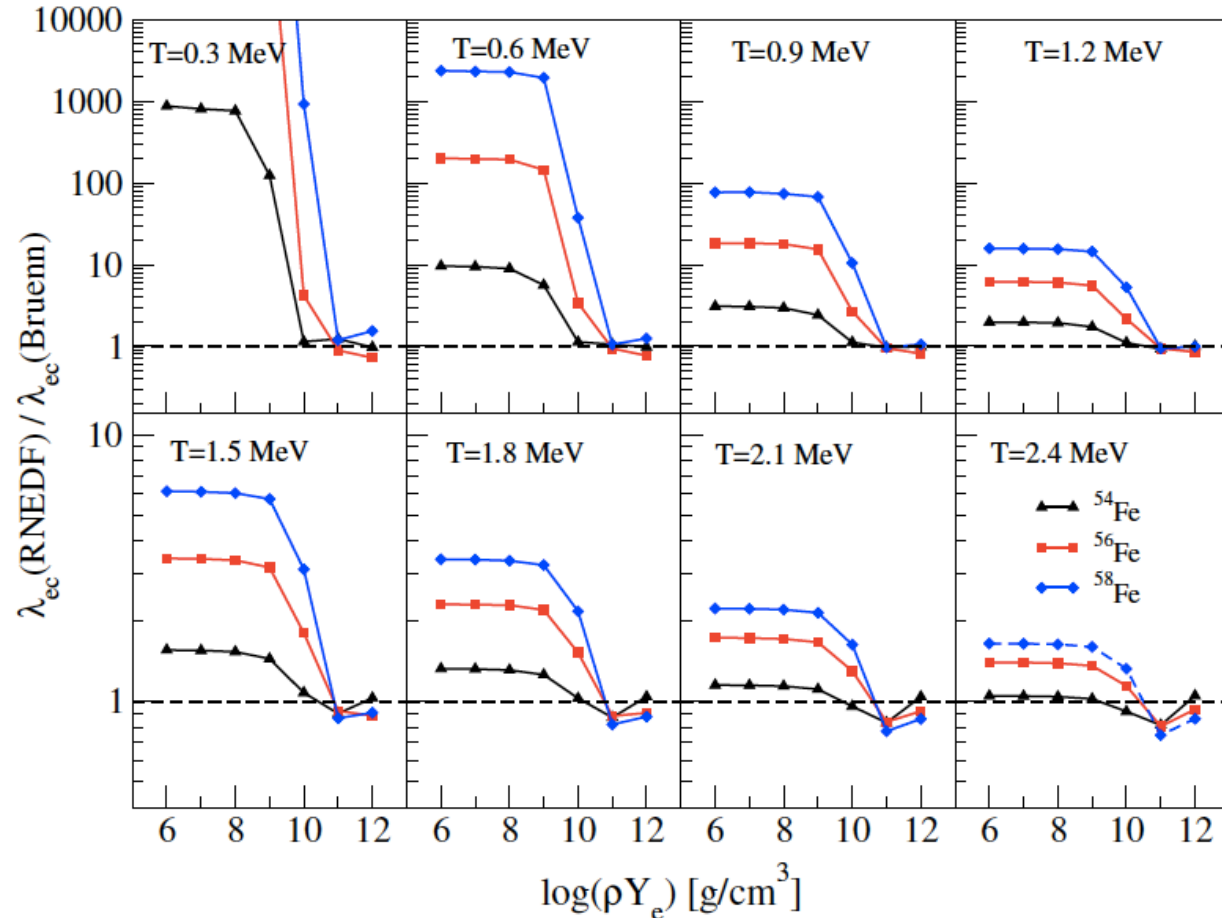


FIG. 7: The ratio between the RNEDF and Bruenn [5] electron capture rates for ^{54,56,58}Fe, shown as a function of ρY_e for the range of temperatures T=0.3,0.6,...,2.4 MeV.

N. P. et al. (2016).
S. W. Bruenn, A.J. Supp. 58, 771 (1985).

Stellar electron capture rates:
RNEDF vs. Bruenn rates

NUCLEAR BETA DECAY

**β -delayed n-emission
branchings
(final abundances)**

**β -decay half-lives
(abundance and
process speed)**

**Seed production
rates ($\alpha\alpha\alpha, \alpha\alpha n, \alpha 2n, \dots$)**

Fission rates and distributions:

- n-induced
- spontaneous
- β -delayed

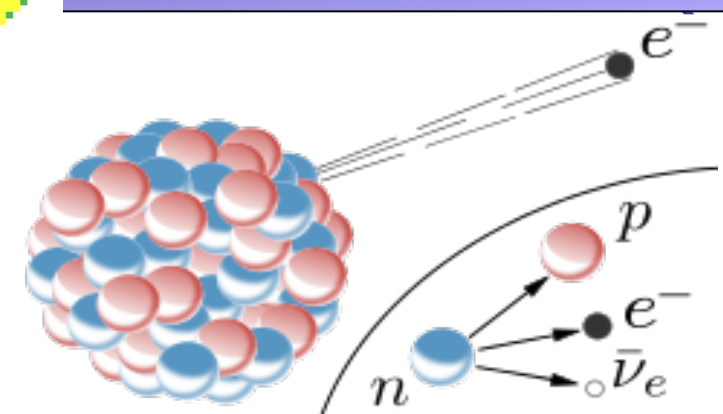
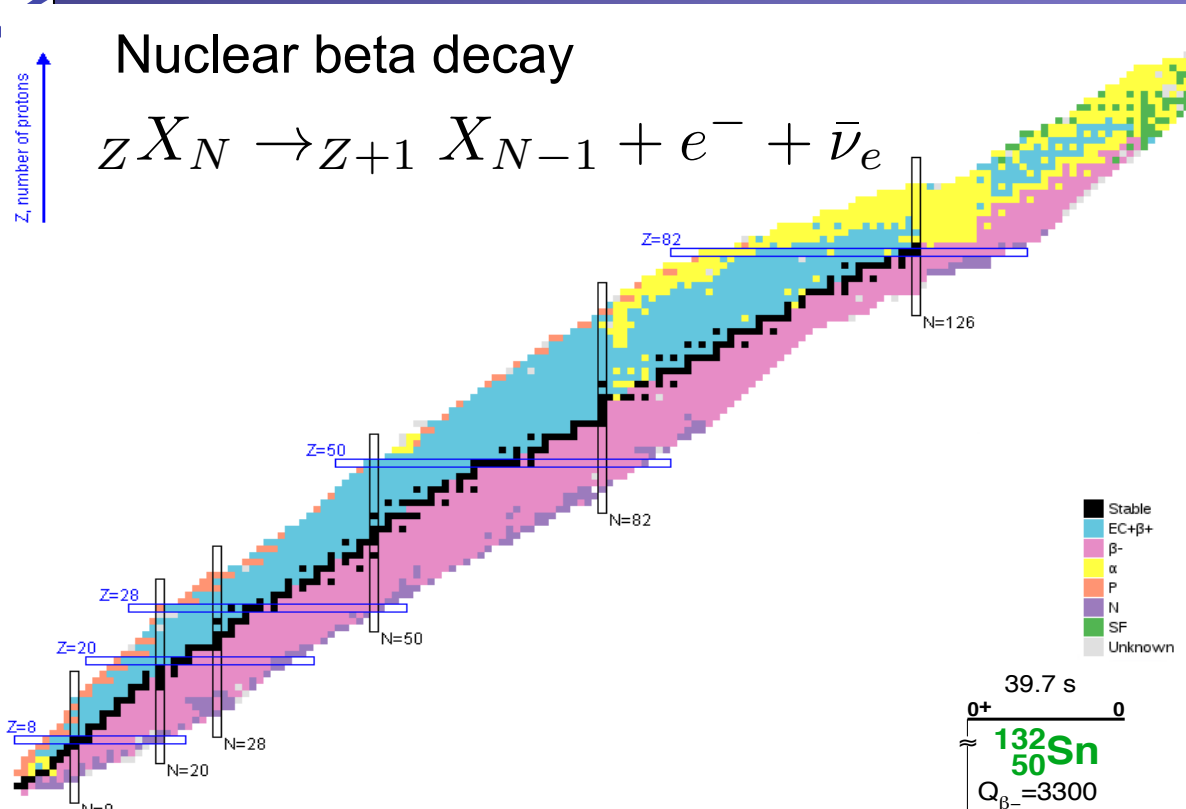
n-capture rates

- for $A > 130$
in slow freezeout
- for $A < 130$
maybe in a “weak” r-process ?

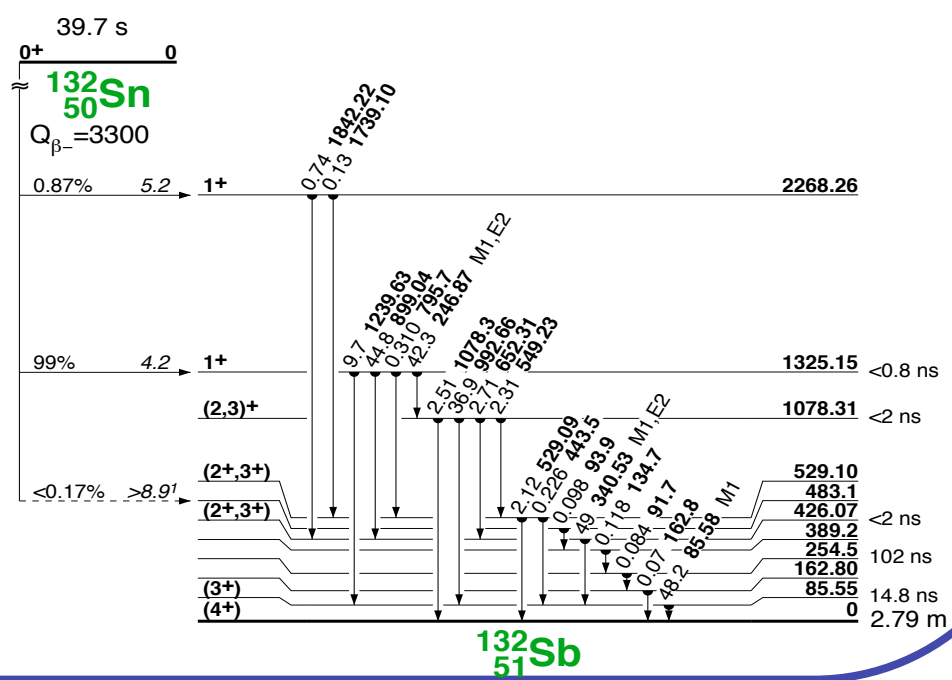
ν -physics ?

**Masses (Sn)
(location of the path)**

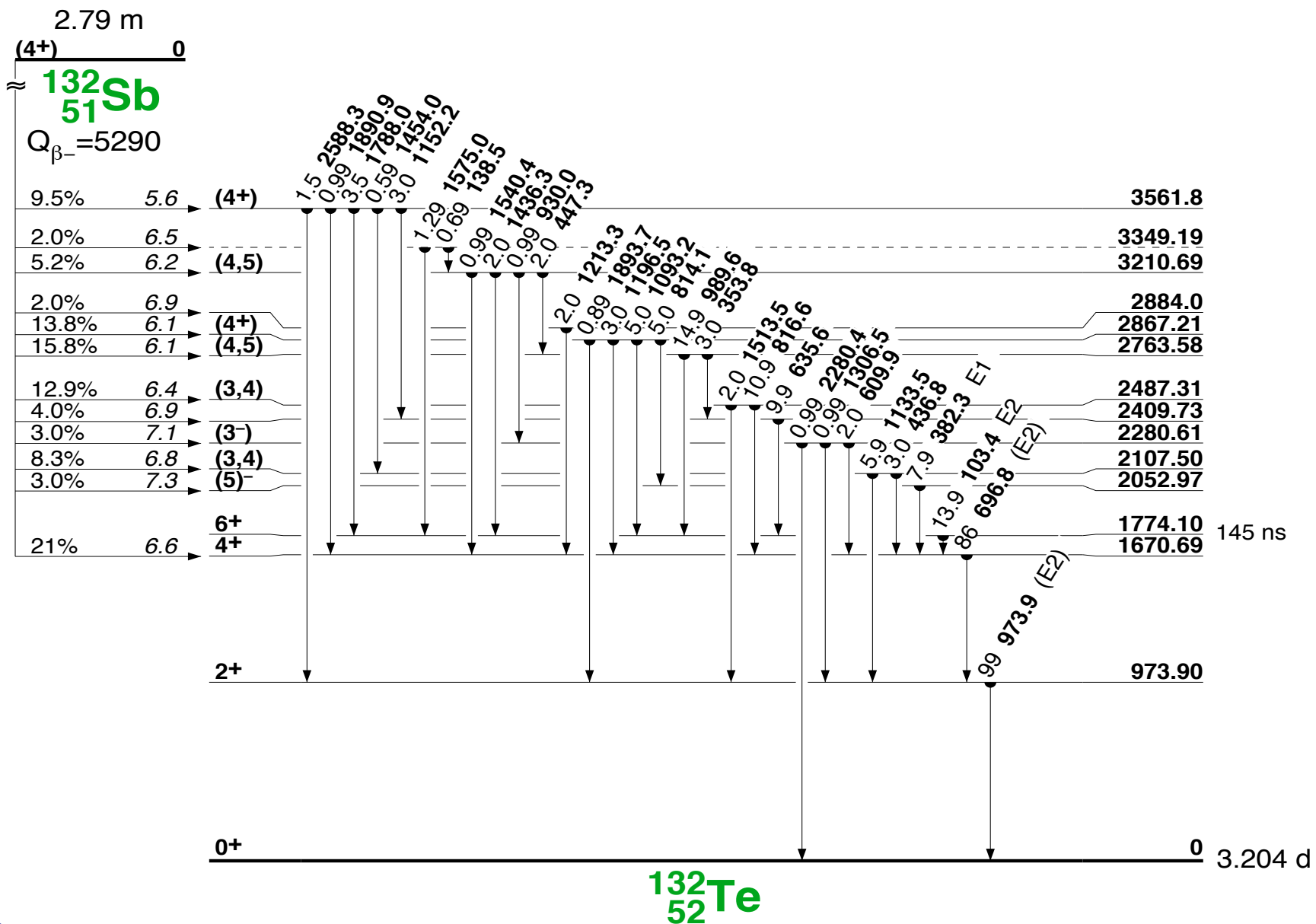
Nuclear beta decay



In some nuclei the decay is quite simple and can be described with just one state.



NUCLEAR BETA DECAY



NUCLEAR BETA DECAY

- Decay rate is of the form

$$\lambda_i = D \int_1^{W_{0,i}} W \sqrt{W^2 - 1} (W_{0,i} - W)^2 F(Z, W) C(W) dW$$

$$T_{1/2} = \frac{\ln 2}{\lambda}, \quad D = \frac{(G_F V_{ud})^2}{2\pi^3} \frac{(m_e c^2)^5}{\hbar}$$

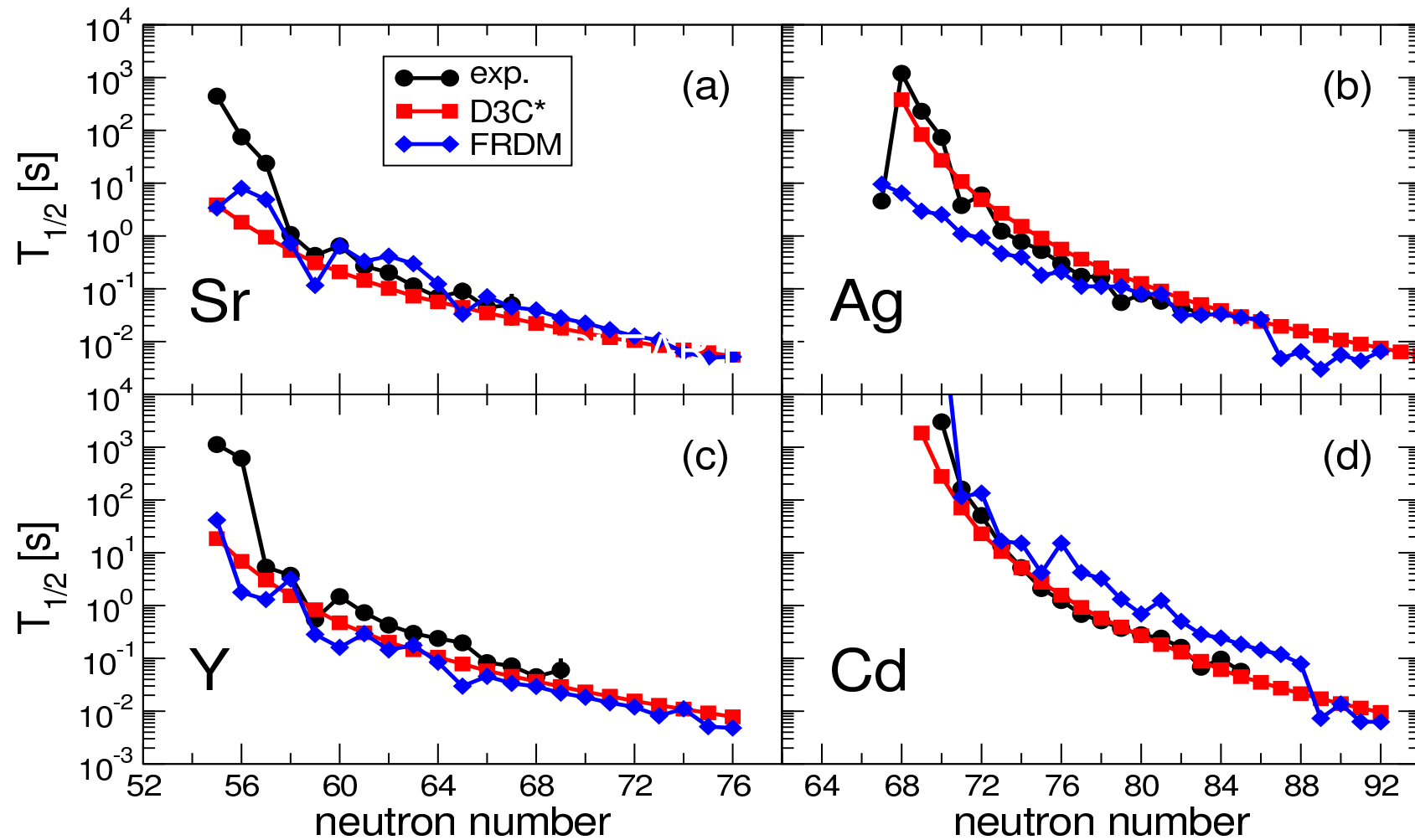
- Allowed decays shape factor:

$$C(W) = B(GT)$$

- First-forbidden transitions shape factor

$$C(W) = k (1 + aW + bW^{-1} + cW^2)$$

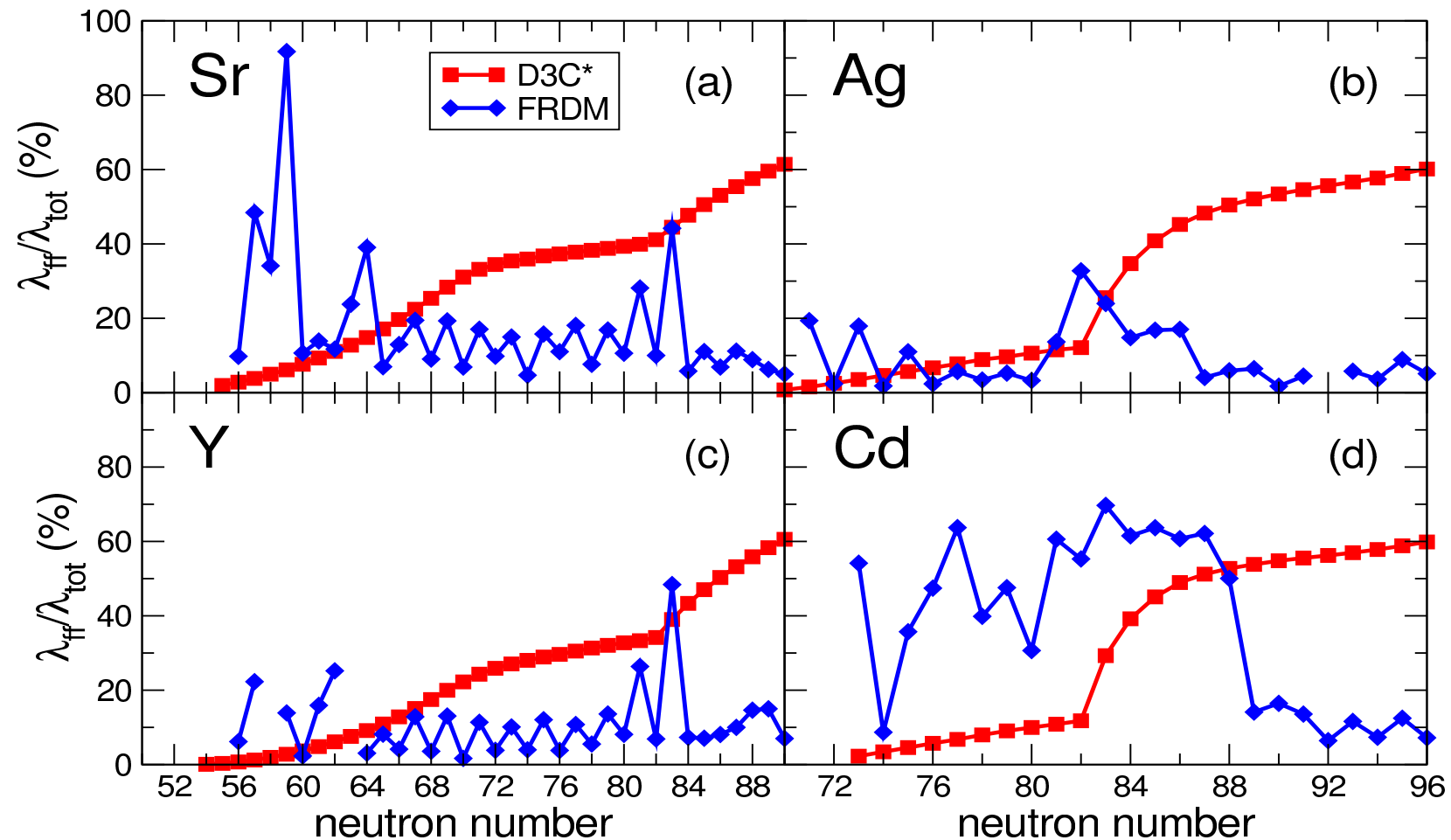
NUCLEAR BETA DECAY



P. Möller, B. Pfeiffer, and K.-L. Kratz, Phys. Rev. C 67, 055802 (2003)
T. Marketin et al., (2016).

NUCLEAR BETA DECAY

- Contributions from the forbidden transitions to the beta decay rates

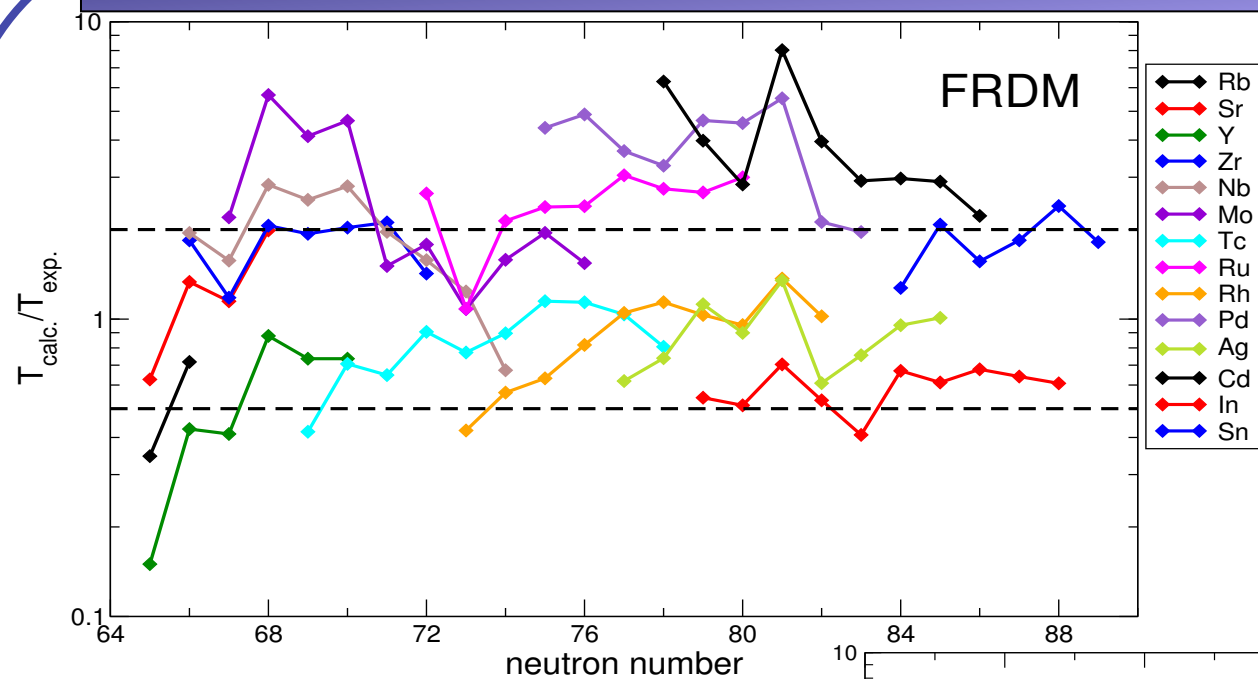


P. Möller, B. Pfeiffer, and K.-L. Kratz, Phys. Rev. C 67, 055802 (2003)

P. Möller, J. R. Nix, and K.-L. Kratz, At. Data Nucl. Data Tables 66, 131 (1997)

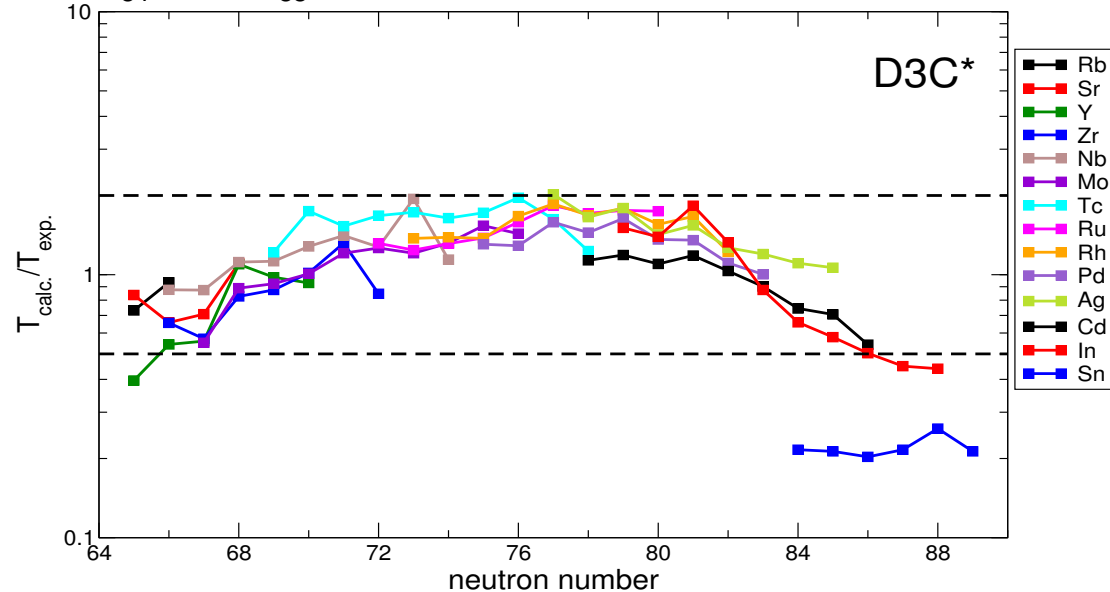
T. Marketin et al., (2016).

NUCLEAR BETA DECAY



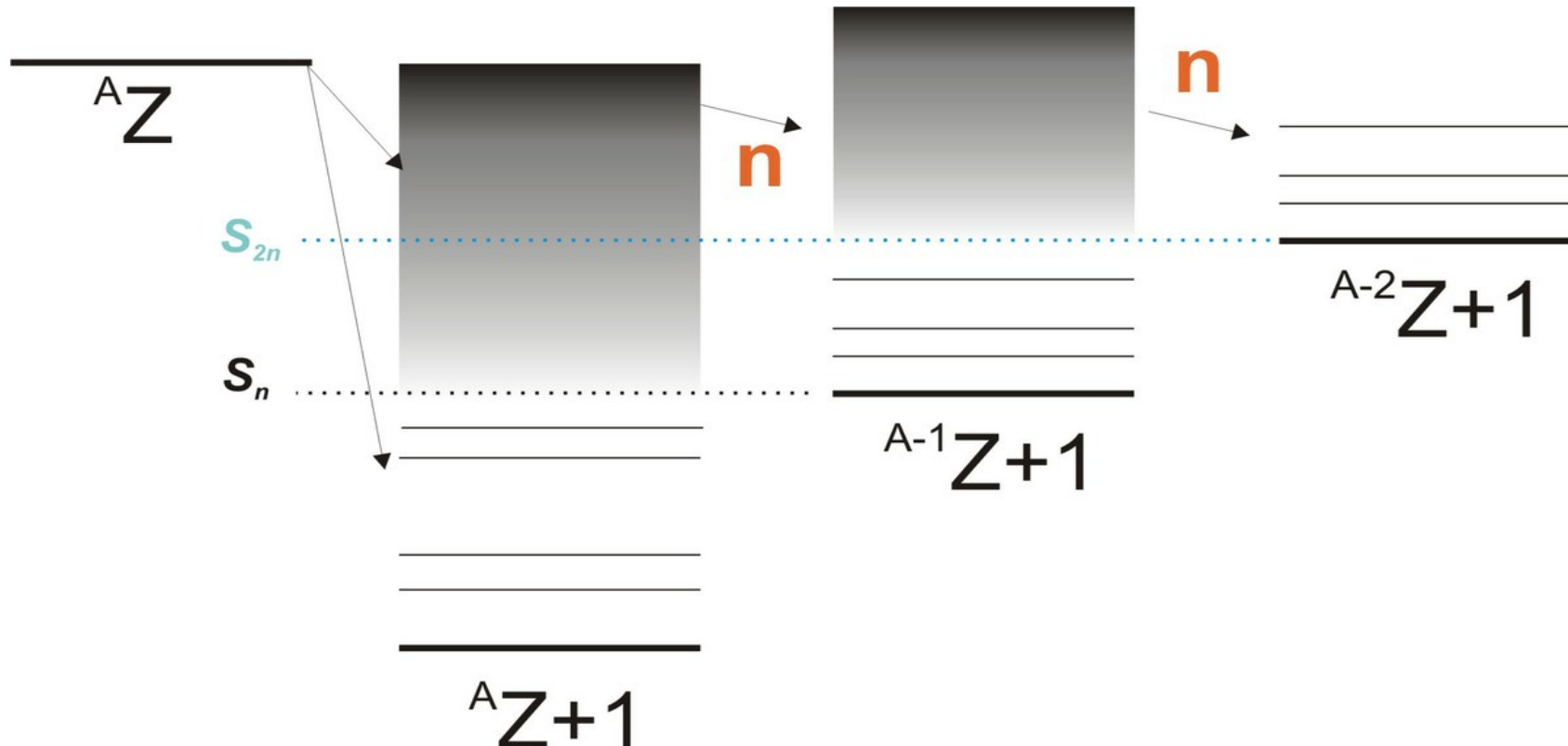
- recent experiment with 110 half-lives
- 40 new measurements

Comparison with the latest measurements is consistent with the previous results.



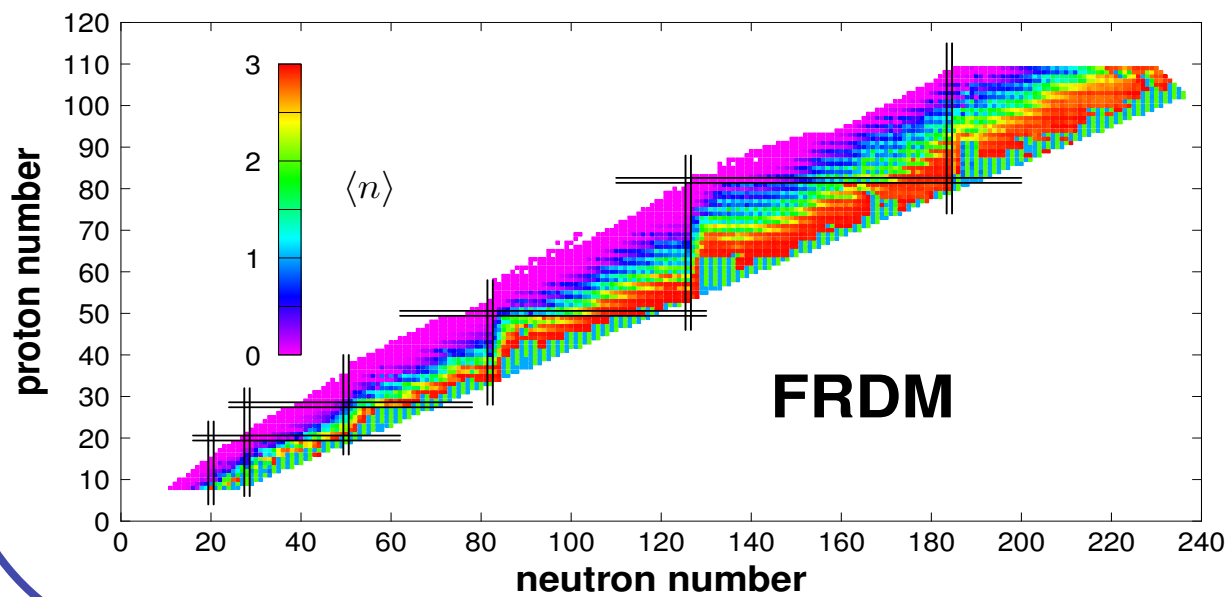
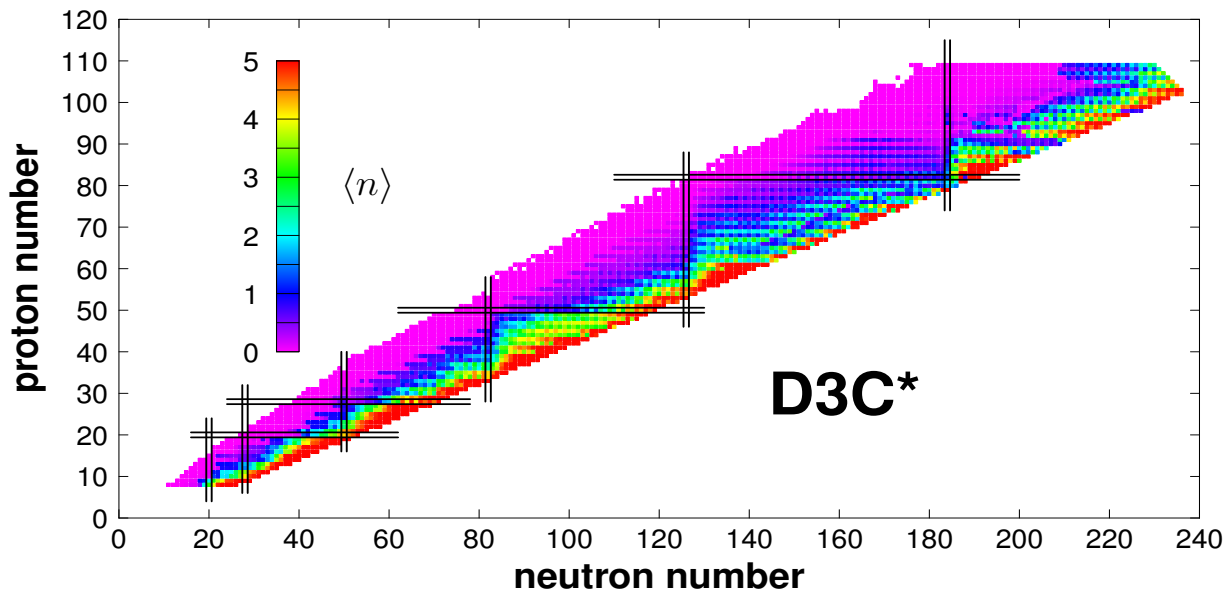
BETA DELAYED NEUTRON EMISSION

In nuclei with small S_n an additional process is possible:
Beta delayed neutron emission



Beta-delayed neutron emission contributes neutrons at the late stages of the r-process, after the initial neutron flux has dissipated.

BETA DELAYED NEUTRON EMISSION

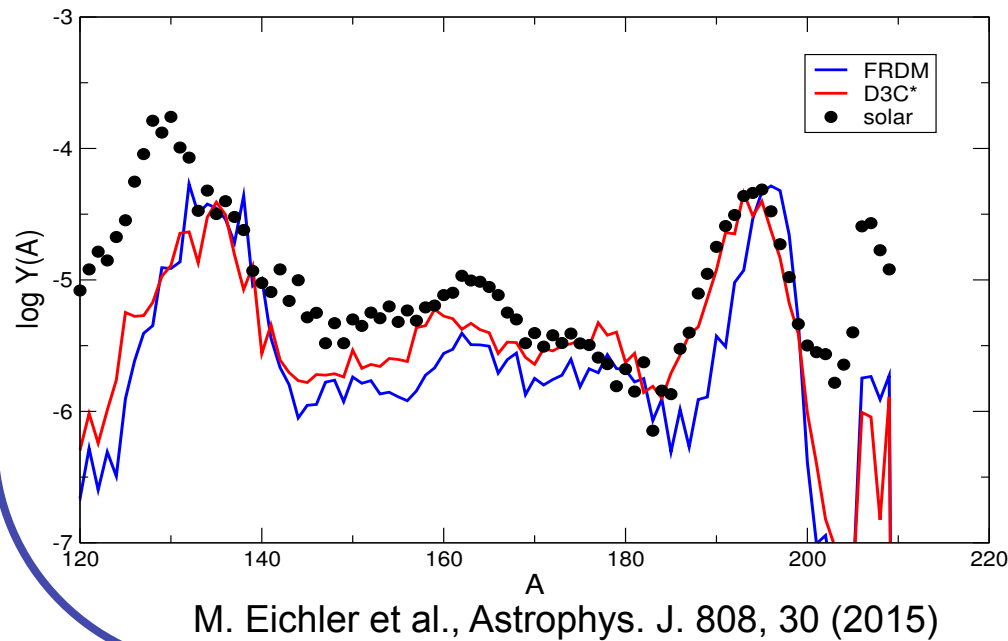


$$P_{xn} = \frac{1}{\lambda_{tot}} \sum_{E_i=S_{xn}}^{S_{(x+1)n}} \lambda_i$$

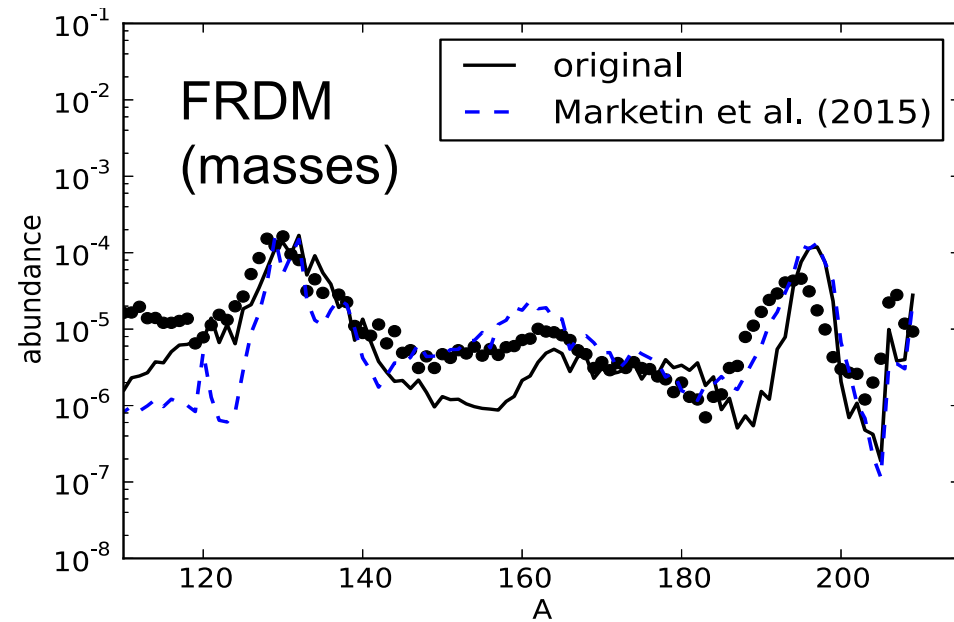
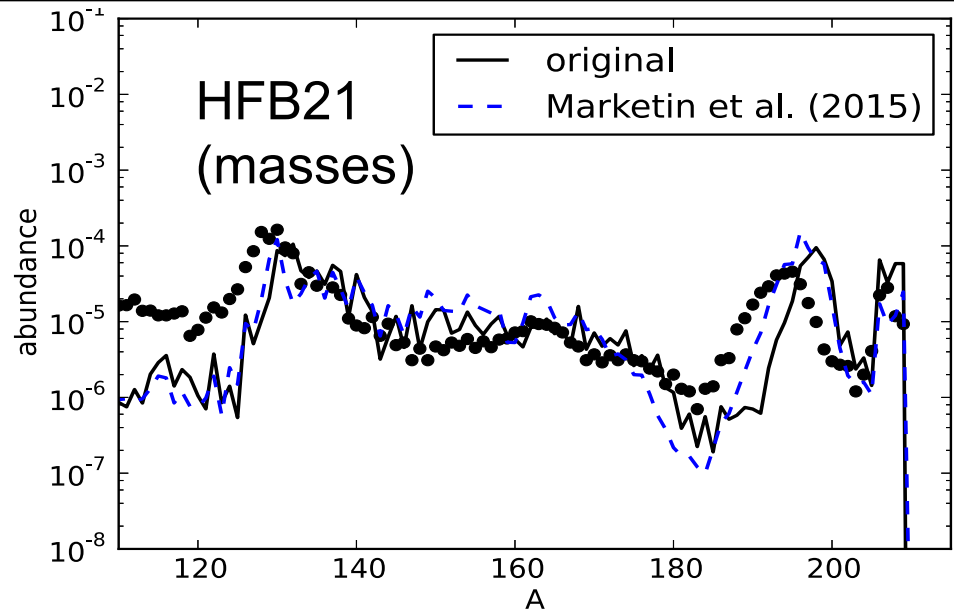
$$\langle n \rangle = \sum_k k \times P_{kn}$$

R-PROCES ELEMENT ABUNDANCES

- half-lives have a significant impact on the abundance pattern
- third peak is particularly sensitive to the changes
- general results for different conditions



M. Eichler et al., *Astrophys. J.* 808, 30 (2015)



FURTHER READING

EDFs, SYMMETRY ENERGY, NEUTRON STARS,...

- J. Piekarewicz et al., PRC 85, 041302(R) (2012)
- A. Krasznahorkay, N. P., D. Vretenar, M. Harakeh, PLB 720, 428 (2013)
- N. P., Ch. C. Moustakidis, T. Marketin, D. Vretenar, G. A. Lalazissis, PRC 90, 011304(R) (2014)
- N. P., D. Vretenar, E. Khan, and G. Colo, Rep. Prog. Phys. 70, 691 (2007).

NEUTRINO-NUCLEUS REACTIONS

- N. P., T. Suzuki, M. Honma, T. Marketin, and D. Vretenar, PRC 84, 047305 (2011)
- H. Đapo, N. P., PRC 86, 035804 (2012)
- N. P., H. Tutman, T. Marketin, T. Fischer, PRC 87, 025801 (2013)
- D. Vale, T. Rauscher, N.P., J. Cosm. Astrop. Phys. 02, 007 (2016)

ELECTRON CAPTURE

- Y. F. Niu, N. P., D. Vretenar, and J. Meng, PRC 83, 045807 (2011)
- A. F. Fantina, E. Khan, G. Colo, N. P., and D. Vretenar, PRC 86, 035805 (2012)
- N. P., G. Colò, E. Khan, and D. Vretenar, PRC 80, 055801 (2009)

BETA DECAYS

- M. Eichler et al., Astrophys. J. 808, 30 (2015)
- T. Marketin, L. Huther, G. Martínez-Pinedo, PRC, to appear (2016)
- T. Marketin, D. Vretenar, P. Ring, PRC 75, 024304 (2007)
- T. Niksic, T. Marketin, D. Vretenar, N. P., P. Ring, PRC 71, 014308 (2005)